Luke Fletcher
Department of Information Engineering, RSISE,
Australian National University
Canberra, Australia
luke.fletcher@anu.edu.au

Alexander Zelinsky
CSIRO ICT Centre,
Canberra, Australia,
alex.zelinsky@csiro.au

Driver Inattention Detection based on Eye Gaze–Road Event Correlation

Abstract

Current road safety initiatives are approaching the limit of their effectiveness in developed countries. A paradigm shift is needed to address the preventable deaths of thousands on our roads. Previous systems have focused on one or two aspects of driving: environmental sensing, vehicle dynamics or driver monitoring. Our approach is to consider the driver and the vehicle as part of a combined system, operating within the road environment. A driver assistance system is implemented that is not only responsive to the road environment and the driver's actions but also designed to correlate the driver's eye gaze with road events to determine the driver's observations. Driver observation monitoring enables an immediate in-vehicle system able to detect and act on driver inattentiveness, providing the precious seconds for an inattentive human driver to react. We present a prototype system capable of estimating the driver's observations and detecting driver inattentiveness. Due to the "look but not see" case it is not possible to prove that a road event has been observed by the driver. We show, however, that it is possible to detect missed road events and warn the driver appropriately.

1. Introduction

The daily occurrence of traffic accidents has become a horrific price of modern life. Complacency about the dangers of driving contribute to the death of more than one million people worldwide in traffic accidents each year (WHO 2001). Fifty million more are seriously injured (WHO 2001). In The Organization for Economic Co-operation and Development (OECD) member countries, road accidents are the primary cause of death for males under the age of 25 (OECD 2006).

There is no doubt that driver error is at the heart of road fatalities (Treat et al. 1979). In their landmark study Neale et al. (2005) used 100 vehicles equipped with video and sensor logging equipment to study how people drive and why they crash. They found that 78% of accidents and 67% of near accidents they witnessed involved momentary inattention (within 3 seconds) before the incident.

We propose to detect and act upon momentary driver inattention. Cars offer unique challenges in human–machine interaction. Vehicles are becoming, in effect, robotic systems that collaborate with the driver. To detect inattention we attempt to estimate the driver's observations in real-time within the vehicle. Through the integration of driver eye-gaze tracking and road scene event detection the driver behavior can be validated against a model of expected behavior to determine cases of momentary driver inattention.

Next, we conduct a brief analysis of the problem of death and injury on the road. In Section 2 we review related work and derive our approach to road safety. Section 3 details system components developed to implement our research. Section 4 describes several inattention detection systems used to verify the efficacy of driver observation monitoring. The paper concludes with a discussion of the next potential steps in road safety in the light of these results.

1.1. Motivation

Law enforcement, improved vehicle and road design and public awareness campaigns have had a marked effect on accident rates since the 1970s (ATSB 2004; OECD 2006). Little, however, has been achieved on the hard cases of road safety, such as fatigue, distraction and inattention (Treat et al. 1979; Stutts et al. 2001; Neale et al. 2005).

The International Journal of Robotics Research
Vol. 28, No. 6, June 2009, pp. 774–801
DOI: 10.1177/0278364908099459

Figures 1–2, 4–6, 8–39 appear in color online: http://ijr.sagepub.com

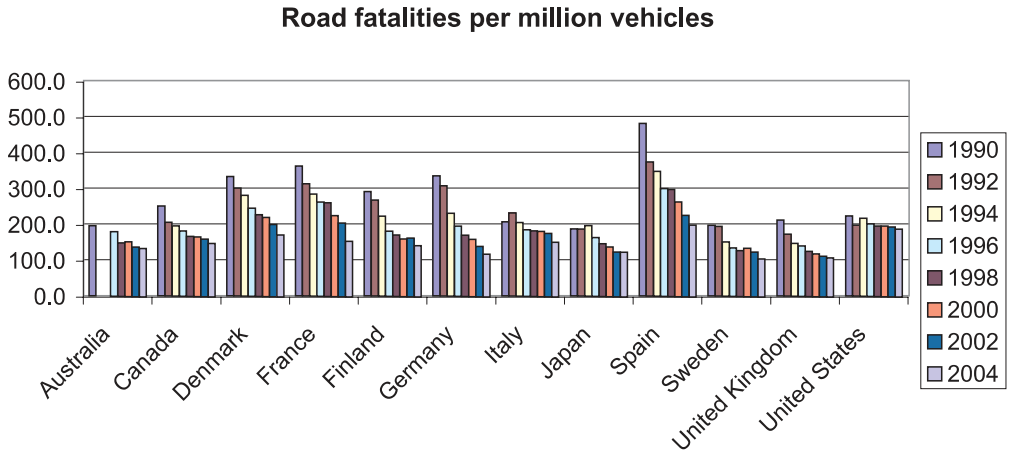

Fig. 1. Road fatalities from 1990 to 2004 per million vehicles across selected OECD countries. Data from OECD (2006).

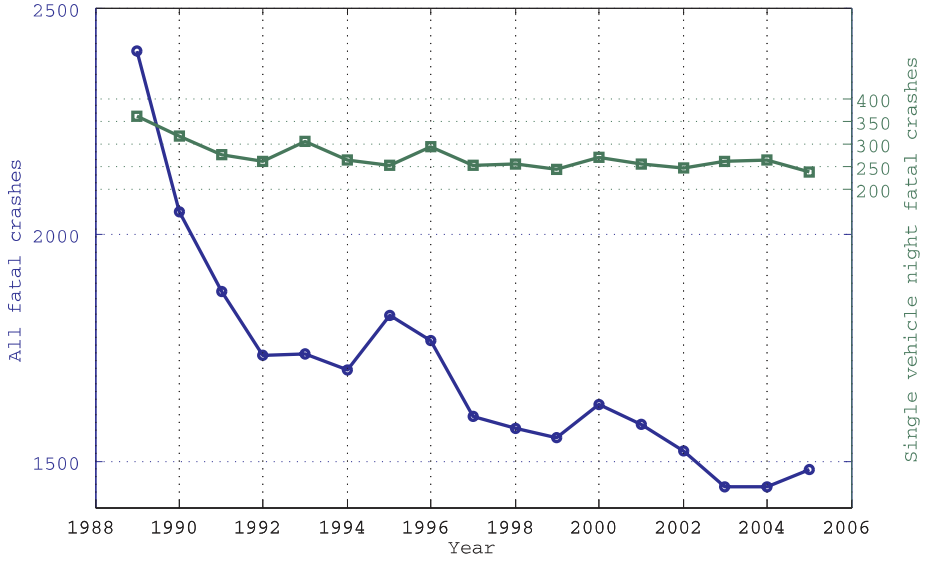

Fig. 2. Fatigue correlated accidents and all fatal crashes. Data from ATSB (2006).

Figure 1 plots the number of road fatalities for several OECD countries over the past 15 years. While many countries such as France and Spain, which were starting from a high base, have steady declines, countries with the lowest fatality rates, such as Sweden and the UK, no longer have a constant decline. Instead, the decrease in fatalities in these countries appears to be slowing (OECD/ECMT 2006). In fact, most OECD countries are losing traction toward the OECD aim of a 50% reduction in road fatalities from 2000 by 2012 (OECD/ECMT 2006).

One reason for this trend is that as road fatalities from speeding and drink-driving fall, the difficult cases in road safety, fatigue, distraction and inattention, are becoming more prominent. To gauge this trend we extracted data likely to correlate well with fatigue-induced accidents from the Australian Road Crash Database (ATSB 2006)[1]. Figure 2 plots night-time single vehicle crashes with the total number of fatal crashes. The plot shows that there is no significant downward trend in (likely) fatigue induced crashes despite a clear downward trend in fatal crashes *per se*.

1. The data extracted was the number of fatal single vehicle crashes during the night (22:00–7:00) compared with the total number of fatal crashes

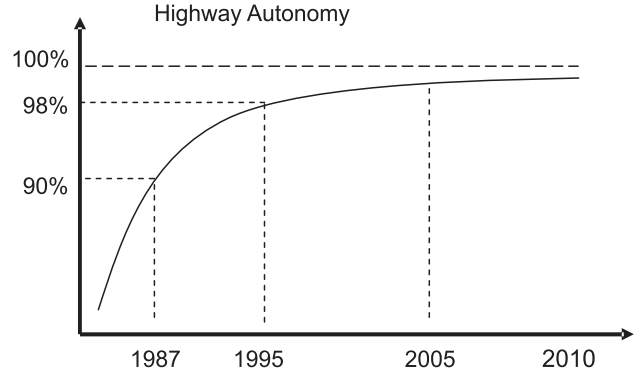

Fig. 3. Diminishing returns of vehicle autonomy. On highways: University of Bundeswehr, Munich (UBM's) "VaMORS" in 1987, Carnegie Mellon University (CMU's) "Navlab 5" in 1995.

It is natural to conclude that the key to eliminating road fatalities is to usurp the failing component, the human driver. There have been a number of impressive feats of autonomous driving. A famous early system pioneered by Dickmanns and Graefe (1988a,b) was able to steer a vehicle at well over 150 km/h on well formed roads. In the 1990s demonstrations of subsequent work in the field were also impressive, e.g. the Navlab "No Hands Across America" trial steered 98% of the 4500 km trip (Pomerleau and Jochem 1996). However, having an automated system address the remaining 2% of road scenarios proved extremely difficult.

As illustrated in Figure 3 autonomous vehicle capabilities have a diminishing return on effort as the capabilities become more advanced. Urban scenes contain substantially more complexity and variance than the highway cases meaning that 100% autonomy in urban and highway scenarios is much further away (Franke et al. 1998). In recent years the United States Defense Advanced Research Projects Agency (DARPA) Grand Challenge, in which road vehicles have been automated to drive in on-road off-road competitions, has generated renewed interest in full vehicle automation (DARPA 2004, 2005). The events while modelled on the "real world" are carefully constrained (DARPA 2007). While challenging to robots the test courses would offer little difficulty to an experienced driver as, again, handling the difficult cases is still a significant time away (Thrun et al. 2006).

Although autonomous technologies in vehicles work very well in their element (over 98% of the time), these systems are highly susceptible to being "tricked" by extreme or unlikely circumstances due to the models they are built on. Humans on the other hand are remarkably flexible. They are able to problem solve on the fly, even when prompted by the most improbable situations. Yet they are susceptible to fatigue, distraction and inattention.

Maltz and Shinar (2004) showed that even an imperfect autonomous technology for driver assistance could provide a significant road safety benefit. So the research agenda shifted to driver support. Here we can use autonomous capabilities to support the driver.

Table 1 summarizes the complementary competencies of a human and an automated driver. Instead of the traditional model of a driver applying the control signal to the vehicle to move through the road environment, we can consider two drivers: the human driver and the autonomous driver, collaborating to control the vehicle. The critical question then becomes how do we combine the behavior of the two controlling agents?

2. Our Approach

Fortunately there is a ready analogy where two drivers are in charge of the one vehicle. Almost every driver has experienced a warning from a passenger, perhaps alerting him or her to an obscured car while merging lanes, or a jaywalking pedestrian in a blind spot. These warnings of inattention save countless lives every day. In a recent keynote address (Regan 2005), Road Safety Researcher Professor Michael Regan[2] highlighted the fact that, unlike other complex, potentially dangerous vehicles such as planes and ships, road vehicles are operated by a single person. That single person is prone to error and may be, due to the day-to-day nature of driving, slow to recognize potential hazards. Professor Regan speculated that the introduction of co-drivers in road vehicles could be the key to a substantial reduction in road accidents.

Our research investigates the implementation of an automated co-driver as a realization of a road vehicle equivalent to aircraft pilot and co-pilot collaboration.

A human aircraft co-pilot provides relief to the pilot by assuming control of the vehicle, but the co-pilot also double checks life-critical actions and shares the burden of administration. We envisage that an Automated Co-driver would provide a role in road vehicles which is an amalgam of a vigilant passenger, driver aid and a safety system. An Automated Co-driver could: double check life-critical actions; relieve the driver of tedious activities; and, crucially, warn about missed road events maximizing the reaction time available for the driver.

2.1. Driver Inattention

Given the high proportion of road accidents that involve inattention, it is our conjecture that the primary contributing factors to road fatalities, speed, drink-driving, fatigue and distrac-

2. Professor Michael Regan is a Research Director at INRETS (The French National. Institute for Transport and Safety Research)

Table 1. Competencies of human and automated drivers.

Human driver	Automated driver
Competent to drive in 100% of road conditions	Competent to drive in 98% of highway conditions
Distractible, inattentive	Vigilant
Susceptible to fatigue	Tireless
Subject to boredom, tedium	Consistent, multitasking, servile
Highly adaptable	Limited programmed behaviour change
High ambiguity and uncertainty tolerance	Limited programmed uncertainty tolerance
Highly evolved yet fixed sensory perception system	Limited yet extendable sensory system, not confined to range of human senses (e.g. millimeter-wave radar)
Limited reaction time	Near instantaneous reaction time

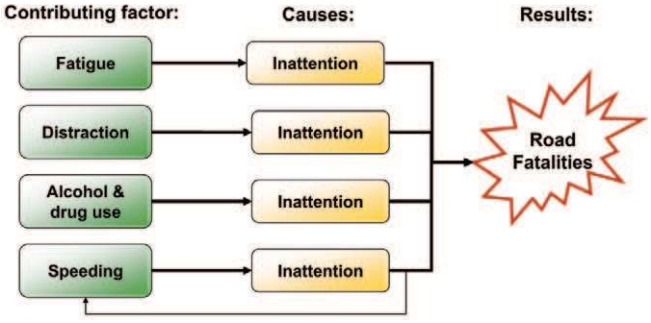

Fig. 4. Accident contributing factors that lead to inattention which leads to road fatalities.

tions, are all actually causes of inattention. The contributing factors all impair the driver's ability to react in time to critical road events. Figure 4 illustrates this point. The primary causes of accidents induce driver inattention which can lead to road fatalities.

By concentrating our efforts on driver inattention interventions, we could break these event chains leading to a substantial reduction of road fatalities across many road scenarios.

2.2. Driver Observation Monitoring

Driver inattention is a highly transient state, and can be due to an identifiable distraction or simply concentration on a competing driving task. Monitoring the vehicle provides knowledge of the vehicle state and the driver's actions. Monitoring the road scene enables us to identify road scene events. However, only driver *inaction*, not inattention, can be estimated using vehicle and road scene monitoring alone. Given a time window of a few seconds, driver inaction detection will occur too late to intervene (Neale et al. 2005). To detect true driver inattention, what the driver has or has not seen must be identified. As illustrated in Figure 5, to detect driver inattention requires accurate real-time driver eye-gaze monitoring combined with vehicle and road scene state.

Our experiments will concentrate on combining driver monitoring with road scene feature extraction to achieve driver observation monitoring.

Direct driver monitoring has been the subject of clinical trials for decades; however, monitoring for use in Advanced Driver Assistance Systems is relatively new.

Head position and eye closure have been identified as strong indicators of fatigue (Haworth et al. 1988). However, when augmented with information about the vehicle and traffic, additional inferences can be made.

Gordon A. D. (1966) conducted an in-depth analysis of perceptual cues used for driving. He described driving as a tracking problem. In on-road systems, Land and Lee (1994) investigated the correlation between eye-gaze direction and road curvature, finding that the driver tended to fixate on the tangent of the road ahead. Apostoloff and Zelinsky (2004) used gaze and lane tracking to verify this correlation on logged data, also observing that the driver frequently monitored oncoming traffic. Ishikawa et al. (2004) explored back projecting the driver's gaze direction onto the scene, but scene features were not identified. Takemura et al. (2003) demonstrated a number of correlations between head and gaze direction and driving tasks on logged data.

Driver monitoring can also be used for validating road scene activity. By monitoring where the driver is looking, usability of the safety system can be improved by suppressing many unnecessary warnings. As long as a road event, such as an overtaking car or wandering pedestrian, is noted by the driver no action needs to be taken.

The behavior of the driver several seconds before and after an important detected road event is used to decide whether to issue a warning. Driver monitoring is achieved via an eye-gaze tracking system and vehicle instrumentation.

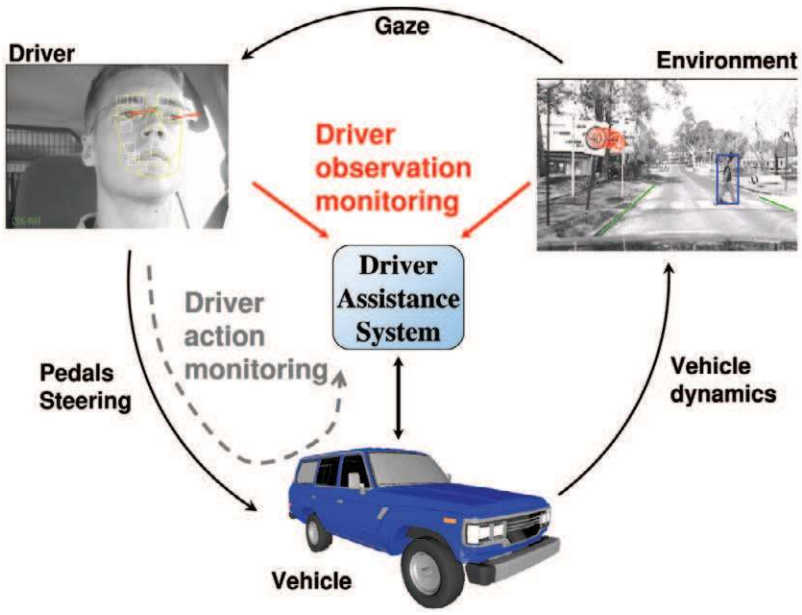

Fig. 5. Driver observation monitoring: driver eye-gaze tracking and critical road scene feature detection are combined to determine what the driver is seeing (or not seeing).

2.3. Autonomous Functions For Driver Support

Many groups have tackled specific sensing and control problems for driver support. A quick survey of the Intelligent Transport Systems (ITS) literature reveals much work in lane tracking/keeping (Dickmanns and Graefe 1988b; Pomerleau and Jochem 1996; Bertozzi et al. 2000), obstacle/vehicle/pedestrian/sign detection (Hsu and Huang 2001; Franke and Heinrich 2002; Labayrade et al. 2002; Grubb and Zelinsky 2004), and driver monitoring (Takemura et al. 2003). However, fewer groups have combined different classes of components to form integrated support systems, with some recent notable exceptions being Takemura et al. (2003), Trivedi et al. (2005) and Holzmann et al. (2006). Interest in integration is emerging with the goals of multidisciplinary networks such as the EU Humanist and AIDE road safety projects (Amditis et al. 2006).

2.4. Vehicle–Driver Interaction

Holzmann et al. (2006) recently outlined an architecture for predictive path planning using a "virtual driver" model, where the driver's actions in addition to other inputs are fed into the driver assistance system. The system, based on its own confidence and the estimated fitness of the driver, generates a safe vehicle control action. No direct driver monitoring seemed to be used. This architecture would be a great complementary component to our system. Gerdes and Rossetter (2001) used force feedback through the steering wheel as a natural human machine interface for lane-keeping. The driver feels a gentle force through the steering wheel encouraging the driver to maintain a central position in the lane. The perception to the driver is that the car is being guided down the lane as if it is on rails, or driving along a trough. The applied force is weak enough, however, that the driver can override the force to overtake or depart. Similarly, Similarly, Carsten and Tate (2001) used feedback through the accelerator for speed control. The accelerator pedal becomes increasingly difficult to depress as the speed limit is exceeded. These interfaces are perfect examples of how a system can give feedback to the driver in a natural unobtrusive way. To permit us to drive on public roads we could not use actuated systems in our experiments. However, these feedback interfaces are how we envisage a final system to operate.

A particularly strong group due to the inclusion of human factors and intelligent vehicle researchers, used a sensor-rich vehicle for driver behavior modeling. Moving from driver behavior analysis to assistance systems the group has recently been correlating driver head pose with road scene perception (Trivedi et al. 2005). They show an improved classification of the driver intent to change lane when head pose data is included in the modeling.

Matsumoto et al. (1999) demonstrated head pose and eye-gaze tracking as a potential human–machine interface. The research has been developed by Seeing Machines (2001) into an in-vehicle system. The system can accurately track head pose and eye-gaze direction down to $\pm 1^{\circ}$. We will use this system to determine eye gaze to correlate with road scene events.

(a) (b)

Fig. 6. (a) The cameras on-board the vehicle. The CeDAR active vision platform containing the stereo road scene cameras and faceLAB^{TM} passive stereo cameras observing the driver. (b) CeDAR: Cable Drive Active vision Robot in vehicle. Four cameras are arranged in two stereo pairs. Cameras are fitted with polarizing filters and far-field cameras use glare hoods.

Using this system, Victor (2005) developed the Percentage Road Centre (PRC) metric which integrates driver eye gaze over time into a histogram to detect driver alertness. The group used a trail of colored lights to lead the driver's attention back to the road when the PRC metric indicated a visual or cognitive distraction preoccupying the driver. Since we are monitoring the instantaneous gaze direction of the driver we prefer not to cause rival visual stimuli to the driving task so we will use auditory messages.

2.5. Judging Driver Behavior

The task of driving is often described as a tracking task (Gordon A. D. 1966; Land and Lee 1994). The driver interprets the road scene primarily by vision and then applies the required control signal to the vehicle to maintain the correct relative position.

Gordon A. D. (1966) reported on a mathematical analysis of the motion of the road scene to the driver. He concluded that, while driving, the road appears in steady state to the driver. Driving then becomes a lateral tracking (lane keeping) problem. Road boundaries, not focus of expansion (as often thought), is the dominant cue for aligning the vehicle in the lanes. If the vehicle is misaligned laterally the whole view field moves as a result. Summala and Nicminen (1996) demonstrated that peripheral vision was sufficient for short-term lane keeping. When the driver is lane keeping the peripheral vision is capable of verifying that small motions in the road scene indicate that the vehicle is on track. When the vehicle starts to diverge from the lane direction, the induced whole view field motion alerts the driver to take direct notice. Correlating the driver eye gaze with the road scene this means that for lane keeping the driver does not always need to fixate on the road for safe driving. However, when the vehicle is misaligned with the road ahead, such as during lane departures, the driver would receive a strong visual cue to monitor the road position. If the driver is not observing the road at this time, then this is a significant indicator of inattention.

This leads to the question of where the driver would look in the road scene for attentive lane tracking. In a clinical trial Land and Lee (1994) investigated the correlation between eye-gaze direction and road curvature. The group found that the driver tended to fixate on the tangent of the road ahead.

Road scene features such as signs, pedestrians and obstacles require foveated vision. Maltz and Shinar (2004) proved that peripheral vision is insufficient for road hazard detection. For our system, this means that to have seen a critical road object the driver must have, at some stage, directed their eye gaze directly at the object.

3. Developed Capabilities

The vehicle has been fitted with sensors to gather odometric information as well as sensors for monitoring the driver's actions such as strain gauges on the steering shaft, turning indicator and brake sensors. The principle sensors used on the vehicle are video cameras. Figure 6 shows the vision systems configuration. Computing is done on-board the vehicle using several standard desktop computers.

3.1. Gaze Monitoring in Vehicles

The vehicle is fitted with a faceLAB^{TM} eye-gaze tracking system. faceLAB^{TM} is a driver monitoring system developed by SeeingMachines (Seeing Machines 2001) in conjunction with

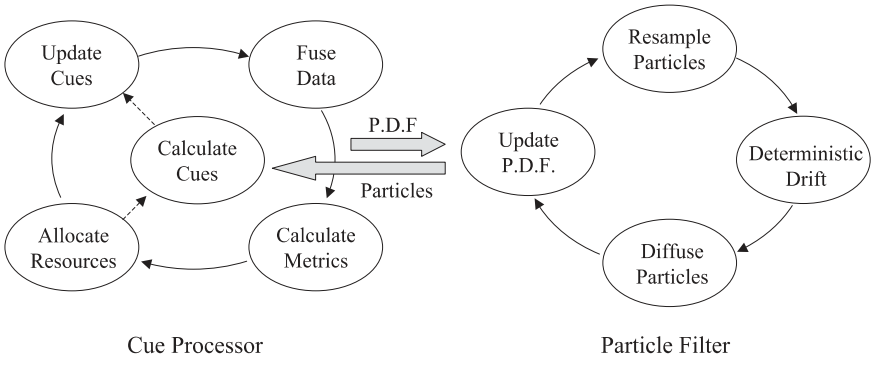

Fig. 7. The Distillation algorithm is composed of a *Cue processor* and a *Particle filter* running concurrently.

the Australian National University (ANU) and Volvo Technological Development. It uses a passive stereo pair of cameras mounted on the dashboard to capture video images of the driver's head. These images are processed in real-time to determine the 3D pose of the driver's head (to ± 1 mm, $\pm 1^\circ$) as well as the eye-gaze direction (to $\pm 1^\circ$). Blink rates and eye closure can also be measured.

3.1.1. Lane Tracking

A common problem in lane tracking is road appearance changes due to shadows, glare and road works (Pomerleau and Jochem 1996; Bertozzi et al. 2000). With the exception of the physical limits of the sensor, in order to achieve robust lane tracking multiple methods of image processing need to be undertaken and integrated based on the prevailing road conditions. The generic *Distillation algorithm* was developed for this purpose. The Distillation algorithm is a visual cue processing framework (see Figure 7). The framework consists of two cycles. The first cycle, the cue fusion cycle, performs a cost–benefit analysis of the various visual cues to *distill* the combination of cues which provide the best tracking discrimination. The second cycle is a particle filter (condensation algorithm (Isard and Blake 1996)) to estimate the state distribution. A detailed discussion of the algorithm is given in Apostoloff and Zelinsky (2004). Figure 7 shows a typical lane estimate, where the initial system has been extended to use a clothoidal road curvature model and a covariance metric is used to incrementally vary the look ahead distance. The lane tracker has been tested on data from a 1800 km round trip tracking the road along a variety of road types without adjustment.

3.2. Obstacle Detection

The Distillation algorithm has also been applied in the obstacle detection system. The obstacle detection system uses a set of visual cues to segment and track obstacles. The detection phase of the system segments potential obstacles from the stereo depth map, edge and motion images. These potential obstacles are very rough guesses with many false positives. These candidates are injected into the Distillation algorithm mentioned above. True obstacles form clusters within the particle space, whereas false detects dissipate. Obstacle samples are defined with respect to the lateral and longitudinal lane positions, size and velocity. While the state space is in world coordinates the sample evaluation is done by projecting back into the sensor image space.

The following equation is used to evaluate each sample:

$$P(e_t^{(j)}|s_t^i) = \frac{1}{\epsilon + N}\left(\epsilon + \sum_p^N I_t^{(j)}(s_p^{(i)})\right), \qquad (1)$$

where $s_p^{(i)}$ is the pth pixel from the set of pixels S generated by particle i, $I_t^{(j)}(s)$ is the value of pixel s from the observation image I used for the jth cue, N is the number of pixels in the region in image space, and ϵ (set to 0.001) is used to support the possibility that the sensor is in error. Figure 9 shows the leading vehicle tracked by the algorithm.

3.3. Sign Recognition

Symbolic signs are detected by locating sign-like shapes in the image stream. The system uses the fast radial symmetry operator (originally developed for eye detection (Loy and Zelinsky 2003)) with online image enhancement. The system was used to effectively detect speed signs as they are the most frequent signs encountered, but a similar method could be used to detect symbolic road signs (Fletcher et al. 2005b). Figure 10 shows the algorithm applied to circular signs in poor road conditions.

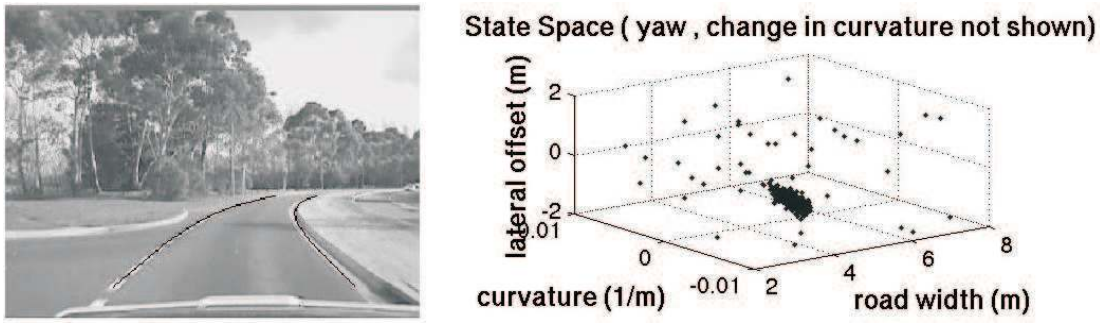

(a) Long look ahead

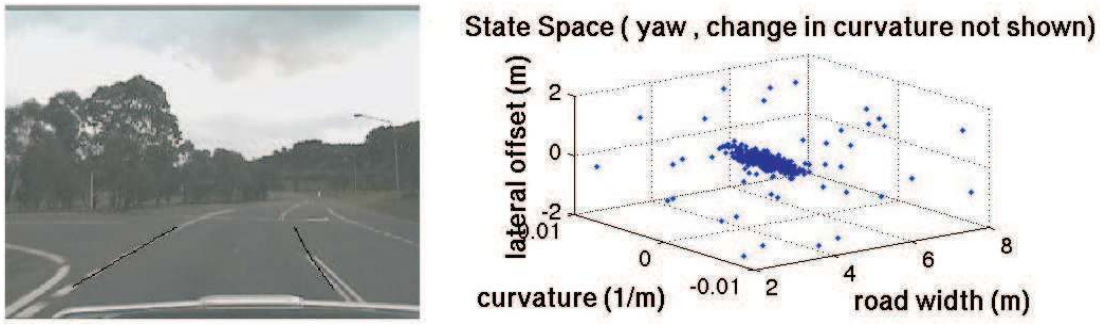

(b) Short look ahead

Fig. 8. Lane tracking look ahead distance varies with certainty measured by the sample spread of the dominant mode.

3.4. Pedestrian Detection

A pedestrian detection system was developed by Grubb and Zelinsky (2004) (see Figure 11). The system used stereo cameras, V-disparity and support vector machines to achieve a high false-negative rate. This system and the work of Viola et al. (2005) has sponsored the development of a second system by our project collaborators, the National ICT Australia group (Rasolzadeh et al. 2006). Viola et al. (2005) implemented a method of detecting pedestrians using Haar features and Ada-boost[3]. The module is used to detect and track pedestrians for our assistance system.

3.5. Visual Monotony Estimation

A great irony of transport systems research is that advances in road and vehicle safety can end up causing new threats to road users. Thiffault and Bergeron (2003) found that the visual monotony is a key input to driver fatigue. Car manufacturers and infrastructure authorities have collaborated to attenuate stimulation from the off-driving tasks and ease the on-driving task. An unfortunate consequence is that sections of road that were once prone, for example, to head on collisions are becoming (after road upgrades) fatigue accident zones.

To automatically measure the visual monotony in a road sequence requires a metric of the variance (or information content) of the video sequence over time. Moving Picture Experts Group (MPEG) encoding fills this requirement. MPEG exploits the property that in moving pictures only small regions of the image actually change substantially between frames. Encoding a set of frames over a sliding time window has shown a strong correlation to a human judged monotony scale. One failing of the MPEG compression as a monotony detector is in situations of poor visibility such as fog. The task was not monotonous yet the video will compress well. We use the lane tracking look ahead distance to detect these types of cases.

We conducted day, dusk and night road trials. To investigate how best to use MPEG encoding to represent monotony we encoded a set of movies with varying sampling rates, ratios and sequence lengths. Figure 12 shows a result of one trial. Trends of smaller compression ratio (or increased monotony) appear as the vehicle leaves the city for the highway and along the country road in day and night trials. The lane tracking look ahead distance is effective at identifying sections of road with a lower monotony than expected by the MPEG compression

3. Ada-boost is a method of taking a collection of weak classifiers and "boosting" them so that together a combination of classifiers is derived that can strongly classify the data set

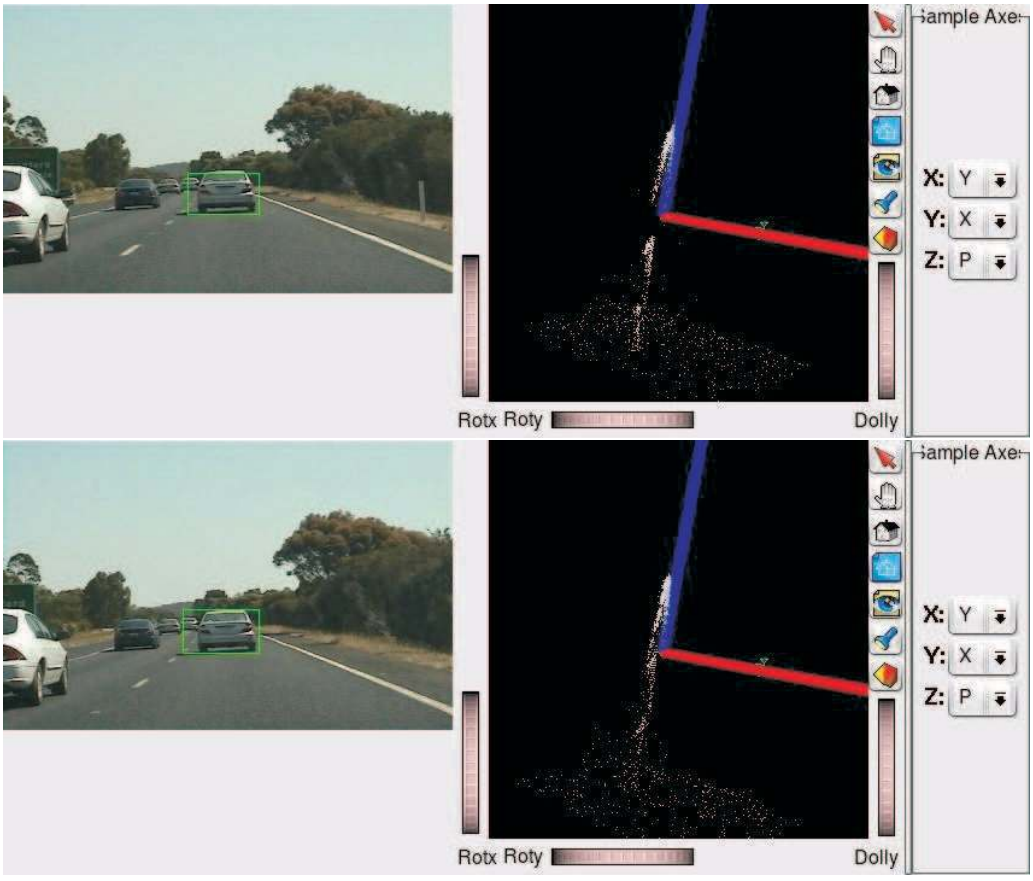

Fig. 9. Distillation algorithm tracking the leading vehicle. Left: Dominant mode projected onto the image. Right: Visualization of the dominant mode in the particle space.

Fig. 10. Sign detection using Fast Radial Symmetry Transform (FRST). The bottom left corner shows the FRST image, where the red crosses highlight detected signs.

alone (Fletcher et al. 2005a). The initial trials were later validated by a 1800 km round trip along a variety of roads and for different traffic types. The metric was highly correlated with the human-perceived monotony.

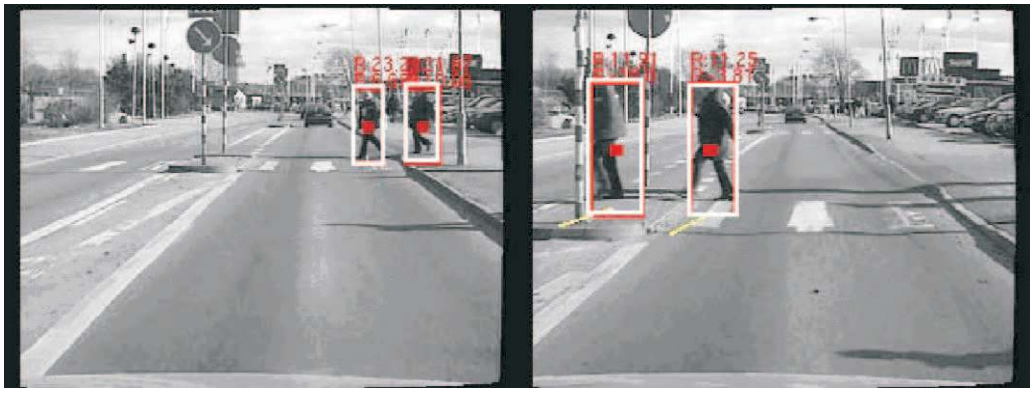

Fig. 11. Online pedestrian detection. The basis for the system used in the Automated Co-driver.

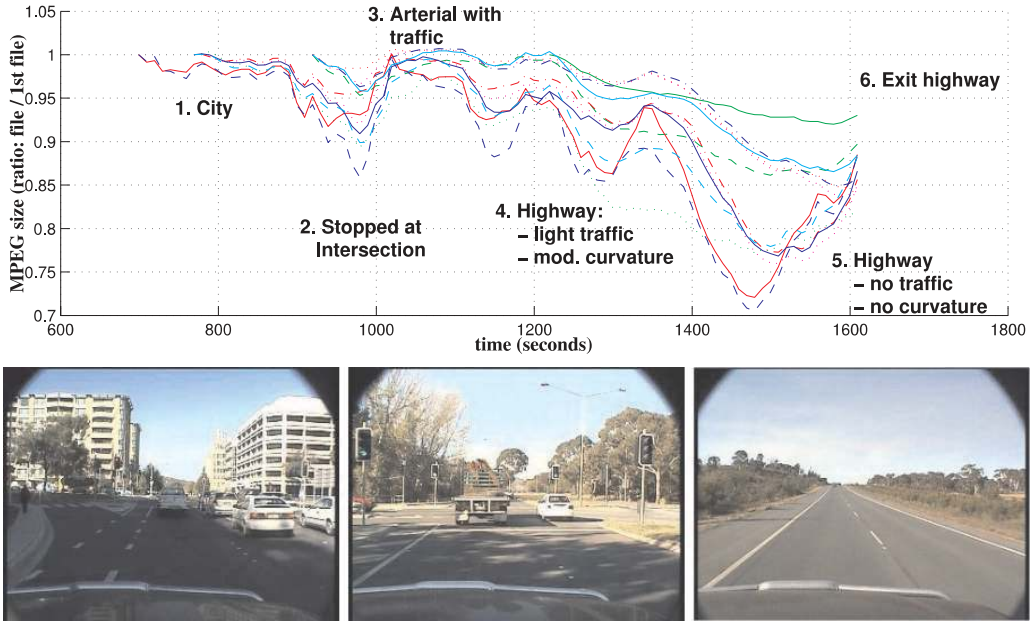

Fig. 12. MPEG compression and lane tracking look ahead during an afternoon trial on city and arterial roads. Sample images from the camera are shown at the corresponding numbered points with the lane tracking look ahead distance. The different traces in the graph represent various frame rate (0.5–4 Hz) and sliding time window (2.5–10 minute) combinations. Higher frame rates capture periodic yet potentially monotonous scenes. Longer time windows smooth transient periods of little motion but add latency to the monotony detection.

4. Driver Inattention Experiments

To investigate driver inattention detection we developed a number of prototype systems:

- *Road center inattention detection* – A simple application using the driver observation monitoring and the vehicle speed alone. This system implements instantaneous driver inattention detection using an assumed road center.

- *Road event inattention detection* – This system integrates a single road event source, namely speed signs, with gaze monitoring to demonstrate the basic cases of driver observation monitoring according to the matrix in Table 2.

Table 2. Driver behavior matrix used by the system to determine the appropriate state. OK: no action required. INFO: provide on-screen reminder to operator. WARN: provide auditory reminder to driver.

Driver	"Seen"	Missed	Acknowledge
Driver Behavior OK	OK	INFO	OK
Driver Behavior Not OK	INFO	WARN	INFO

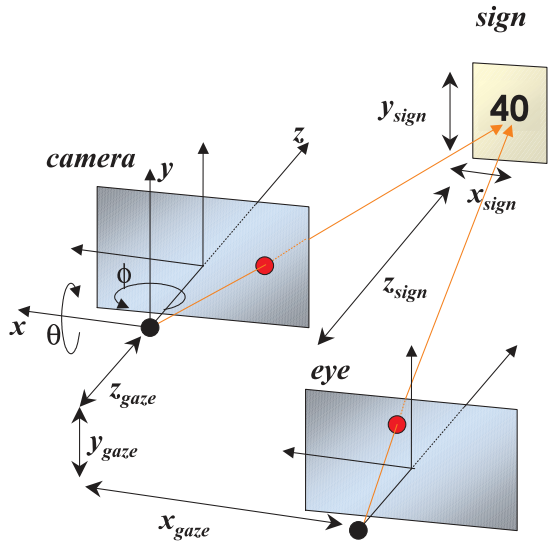

Fig. 13. The scene camera and gaze direction is analogous to a two-camera system.

- *Multiple road event inattention detection* – The final system integrates all available subsystems to demonstrate our best approximation of a fully functional driver inattention detection system.

Our approach is to consider the driving task as a closed loop system involving the vehicle, driver and the road environment. The system selected interventions according to the behavior matrix in Table 2.

4.1. Correlating Eye Gaze with the Road Scene

Scene camera and eye configuration is analogous to a two-camera system (see Figure 13). Gaze directions trace out epipolar lines in the scene camera. If we had a depth estimate of the driver's gaze, we could project to a point in the scene camera. Similarly, if we had the object depth we could re-project on to the eye and estimate the required gaze. A depth estimate of the gaze is hard to obtain. A common assumption is that the gaze angle and angle in the scene camera are the same. In practice this assumption amounts to supposing that either the scene camera is sufficiently close to the driver's head (equivalent to a trivial baseline) or that the objects of interest are near infinity (Land and Lee 1994; Takemura et al. 2003; Ishikawa et al. 2004). In these cases error bounds on the gaze direction (not fixation duration) are infrequently used and even less frequently justified.

The object depth could be estimated using a second scene camera running the same detection software or assumptions on object size and/or road layout. However, it is desirable to maintain flexibility of the implemented object detection systems which could use a single camera and have no strong assumptions on the object scale. If we assume that the depth of the object is unknown, we can instead model the effect of the disparity error in our confidence estimate.

The effect of an unknown stereo disparity will be a displacement along the epipolar line defined by the gaze direction on to the scene camera. The disparity, as with any stereo configuration, will be most apparent for close objects and reduce by a $1/x$ relationship with distance from the baseline. The angular deviation reduces as the angle becomes more obtuse. To get an upper bound of the likely disparity deviation we can compute the worst-case disparity for our camera configuration. With reference to Figure 13, and using the scene camera center as a world reference frame, the scene camera and gaze angles for a sign at $(X_{sign}, Y_{sign}, Z_{sign})$ can easily be derived:

$$\begin{aligned}\Delta\theta &= (\theta_{cam} - \theta_{gaze}) \\ &= \arctan\frac{X_{sign}}{Z_{sign}} - \arctan\frac{X_{sign} + X_{gaze}}{Z_{sign} + Z_{gaze}}, \qquad (2)\\ \Delta\phi &= (\phi_{cam} - \phi_{gaze}) \\ &= \arctan\frac{Y_{sign}}{Z_{sign}} - \arctan\frac{Y_{sign} + Y_{gaze}}{Z_{sign} + Z_{gaze}}. \qquad (3)\end{aligned}$$

The worst-case disparity then translates to when the object is closest to the vehicle on the driver's side of the road, equivalent to an object on the right shoulder of a single-lane road (note that our system is in a right-hand drive vehicle). The field of view of the scene camera limits the closest point at which the object is visible. The closest visible object is at $(-3.0, -1.6, 8.0)$ for the 50° field of view of the camera. The worst-case height of the object relative to the scene camera, -1.6, would be when it is on the ground (this is worse than any actual case as the object would not be visible due to the bonnet). With pessimistic estimates of the driver (far) eye position relative to the scene camera manually measured to be $(X_{gaze} = 0.22, Y_{gaze} = 0.1, Z_{gaze} = 0.2)$, the final errors become

$$\Delta\theta = (\theta_{cam} - \theta_{gaze}) = (20.6^\circ - 18.7^\circ) = 1.9^\circ, \quad (4)$$

$$\Delta\phi = (\phi_{cam} - \phi_{gaze}) = (11.3^\circ - 10.4^\circ) = 0.9^\circ. \quad (5)$$

Therefore, the worst expected deviation due to stereo disparity is $\pm 1.9^\circ$ horizontally and $\pm 0.9^\circ$ vertically, which is on a par with other error sources in the system. The expected deviation for the majority of cases where the sign is further away is significantly less. The deviation is twice as large in the horizontal direction, implying that a suitable approximation of the tolerance region will be an ellipse with a horizontal major axis.

To determine the overall tolerance of the system, two further factors need to be accommodated. The gaze tracking system has an accuracy of $\pm 3^\circ$ and the field of view of the foveated region of the eye is estimated to be around $\pm 2.6^\circ$ (Wandell 1995). The accumulated tolerance is the sum of these sources which for our experimental setup comes to $\pm 7.5^\circ$ horizontally and $\pm 6.6^\circ$ vertically. This allows us to claim that the driver was very unlikely to have seen the object if the object and gaze directions deviate by more than this tolerance.

Verifying the Foveated Field of View

To get a sense of the field of object discrimination ability of the driver, a simple trial was constructed using a desktop PC. Wandell (1995) states the foveated region of the eye to be around $\pm 2.6^\circ$, although a substantial cone density exists up to around 20°. A simple program was made to present speed signs featuring varying speeds to the subject at different positions on the screen. Highway road footage was shown in the background to add a small amount of realism to the scene. The test subject was asked to fix their gaze on a stationary cross on the screen and to press the corresponding number on the keypad to match the presented sign. If the subject broke their gaze or otherwise invalidated the trial, they pressed no key or "0" and the result was discarded. Figure 14 presents a typical screenshot from the test program. A set of five subjects with normal (or corrected) eye sight were each presented with 200 signs (100 fixating to the left, 100 fixating toward the right). The results (see Figure 15) show that reliable discrimination ability drops off at over 4° from the fixation point. The use of the trial was to provide a rule of thumb for the discrimination ability of the driver in the context of the road objects. The estimated field of discrimination will be used to judge whether the driver would be able to see a particular road object.

In-vehicle Verification

We conducted a verification experiment to test that the system was indeed going to be able to detect whether the driver missed an object. The driver was asked to fix their gaze on an object in the scene. A sign was then placed at a certain distance from the fixation point. The driver was then asked to identify the object. The object was one of eight possibilities. The proportion of correct classifications was logged along with the driver-gaze angle and apparent sign position in the scene camera. 30 m, 20 m and 10 m depths were tested against four different displacements between the object and fixation point. The object size was 0.45 m in diameter. For each combination of depth and displacement, ten trials were done.

Fig. 14. Screen-shot of PC test application to gather data on gaze object recognition field of view. A test subject is requested to fix their gaze on the cross. The Speed sign periodically varies in position and speed (10,20,30,...,90). A road video sequence was played in the background to add context for the trials. The subject entered the "guessed" sign via a numeric keypad ("1"–"9").

Figure 16 shows the driver's object classification error rate versus the angle between gaze and object position. Expected recognition rates fall as the object becomes more peripheral in the driver's field of view. The results of this trial verify our expectation that, while it is hard to prove the driver saw an object, it is possible to estimate, with reasonable confidence, when the driver was unlikely to have seen the object. A curious effect was noticed (represented by a cross in the middle of the graph) when the driver was very close to the object. The large apparent size of the object in the driver's field of view seemed to aid the recognition rate. However, this only occurred when objects were close to the vehicle, which is not when drivers typically see road objects. The driver reported not consciously being able to see the object in this case.

This verification demonstrates the expected strength of the system: the ability to detect when the driver has missed an object. It is impossible to determine whether the driver saw the object, as, even with perfect measurement of a perfect gaze direction match, the driver's attention and depth of focus cannot be determined. If the driver is looking in the direction of the object, it is an ambiguous case whether the driver noticed the object, thus no warning is issued.

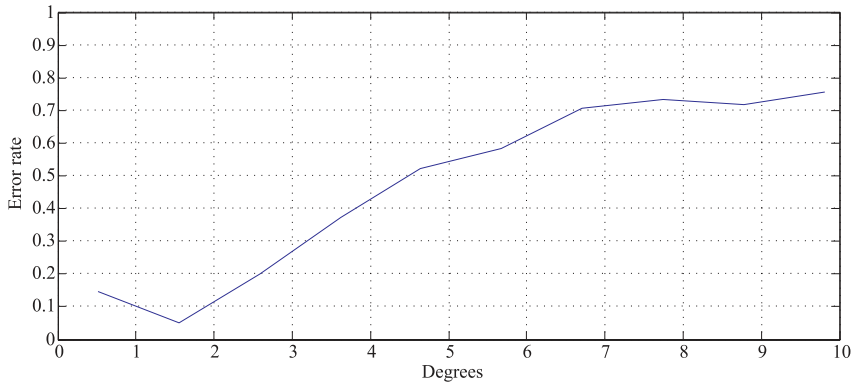

Fig. 15. Gaze PC test error rate. Above a 4.5° angle from the fixation point the test subjects were recognizing one in two signs correctly.

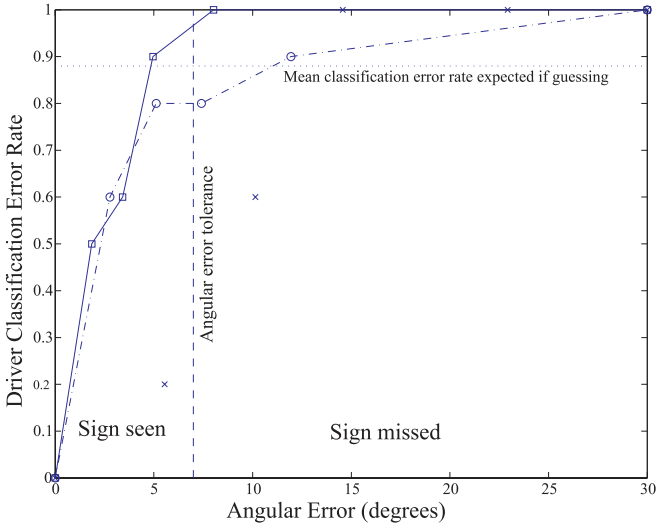

Fig. 16. Driver recognition rate of objects in peripheral vision for various depths. The dotted horizontal line shows expected value due to chance. The vertical dashed line represents ±7.5° derived tolerance. Squares, 30 m points; circles, 20 m points; crosses, 10 m points.

4.2. Assistance System Design

The Automated Co-drivers can be thought of (and are implemented) as instances of the Advanced Driver Assistance Systems (ADAS) logic engine shown in Figure 17.

4.3. Road Centre Inattention Detection

The first system was developed to demonstrate the benefits of the immediacy of direct driver gaze monitoring. Previous systems used in simulation or road trials have used metrics such as the variance in steering wheel movements to gauge the fatigue level of the driver. Because these systems compute statistics over time, there is a significant lag between driver inattention and action by the system. Online real-time driver gaze monitoring can easily be used to detect short periods of driver distraction.

Similar to the percentage road center metric (Victor 2005), driver gaze can be analyzed to detect even shorter periods of driver distraction. The faceLAB^{TM} system readily allows the implementation of an online distraction detector. The gaze direction is used to reset a counter. When the driver looks forward at the road scene, the counter is reset. As the driver's gaze diverges, the counter begins. When the gaze has been diverted for more than a specific time period, a warning is given. The time period of permitted distraction is a function of the speed of the vehicle. As the speed increases, the permitted time period could drop off either as the inverse (reflecting time to impact) or the inverse squared (reflecting the stopping distance). We use the inverse square. Once the driver is observed to have had a stable gaze at the road ahead, the counter and the warning is reset until the next diversion. As the vehicle speed is considered, normal driving does not raise the alarm since dramatic movements such as over the shoulder head checks occur at slow speeds, and the overted gaze tolerance is longer. Situations when the vehicle is not moving, such as waiting to merge, permit the driver to look away from the road ahead indefinitely without raising the alarm.

Using the faceLAB^{TM} system, we monitor driver head pose and eye-gaze direction via the driver state engine. The watchdog timer inside the driver state engine will be used to verify whether the driver has not looked at the road for a significant period of time. An auditory warning is given if the driver is seen to be inattentive.

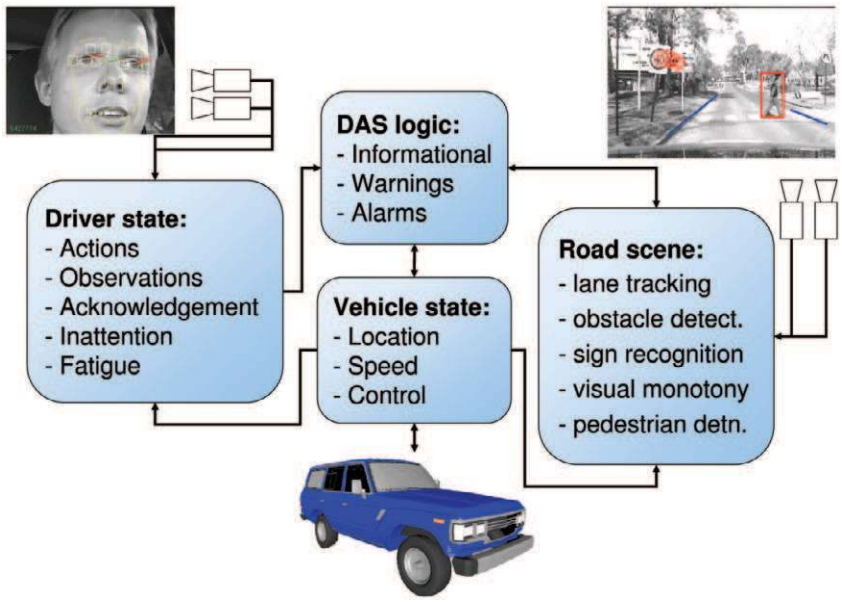

Fig. 17. Implemented ADAS software component architecture.

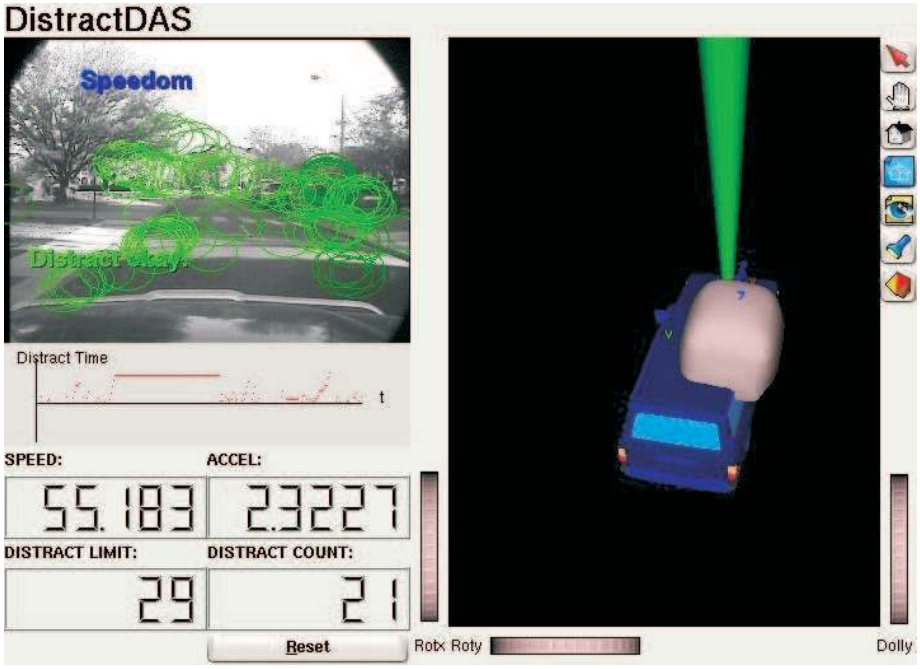

Fig. 18. Road scene inattention detection Automated Co-driver screen-shot.

On-road Trials

Figure 19 is a sequence of screen-shots showing the typical response with a distracted driver. Once the distraction threshold is crossed for the given speed, audio warnings increase until the driver looks forward again. Then the warnings are reset until next time. One conclusion from the trials was that a road position estimate would help the system. In some cases, when the road had significant curvature, the system was triggered because the gaze direction was substantially away from the straight ahead position.

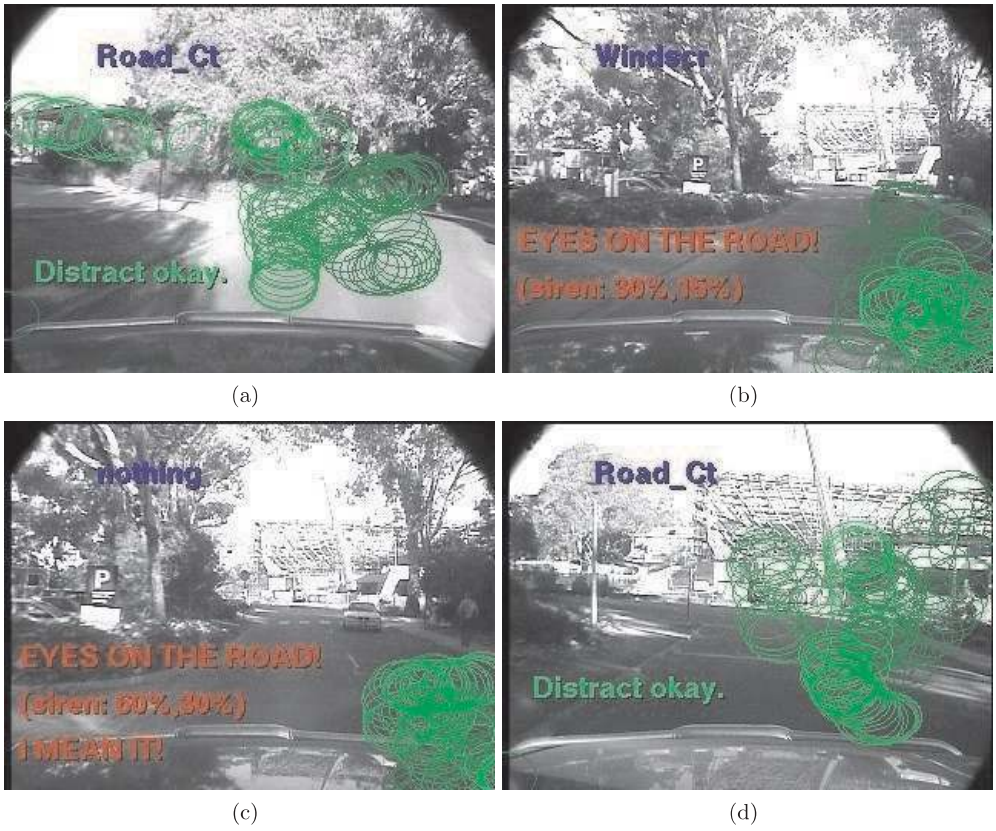

Fig. 19. Road scene inattention detection sequence. Circles represent driver gaze. (a) Driver looking forward. (b) Driver looking at right mirror, alarm sounding. (c) Driver still distracted, alarm louder. (d) Driver gaze has returned to the road ahead, alarm silenced.

4.4. Road Event Inattention Detection

In this system an autonomous detection system recognizes a road event, in this case a speed sign. At the same time, a driver monitoring system verifies whether the driver has looked in the direction of the road sign. If it appears that the driver is aware of the road sign, the information can be made available passively to the driver. If it appears that the driver is unaware of the information, an auditory warning is generated.

For this case, if the driver appears to have seen a speed sign, the current speed limit can be simply recorded on the dashboard adjacent to the speedometer. However, if it appears that the driver has not looked at the road sign and, over time, a speed adjustment is expected and has not occurred, a more prominent warning would be given. This still leaves the driver in control of the critical decision, but supports them in a way that aims not to be overly intrusive. Warnings are only given when the driver is not aware of the change of conditions. Finally, the warning can also be cancelled by observing the driver: a glance at the speedometer confirms that the driver is aware of their speed and the new detected limit.

Using the reasoning in Section 4.1, the worst expected deviation due to stereo disparity is $\pm 1.9^\circ$ horizontally and $\pm 0.9^\circ$ vertically which is on a par with other error sources in the system. The expected deviation for the majority of cases where the sign is further away is significantly less. The deviation is twice as large in the horizontal direction, implying that a suitable approximation of the tolerance region will be an ellipse with a horizontal major axis.

To determine the overall tolerance of the system, two further factors need to be accommodated. The gaze tracking system has an accuracy of $\pm 3^\circ$ and the field of view of the foveated region of the eye is estimated to be around $\pm 2.6^\circ$ (Wandell 1995). The accumulated tolerance is the sum of these sources, which for our experimental setup comes to $\pm 7.5^\circ$ horizontally and $\pm 6.6^\circ$ vertically. This allows us to claim that the driver was very unlikely to have seen the sign if the sign and gaze directions deviate by more than this tolerance.

To correlate the eye gaze with the sign position, the histories of the two information sources are examined. The sign detection sub-system provides a history of the sign location

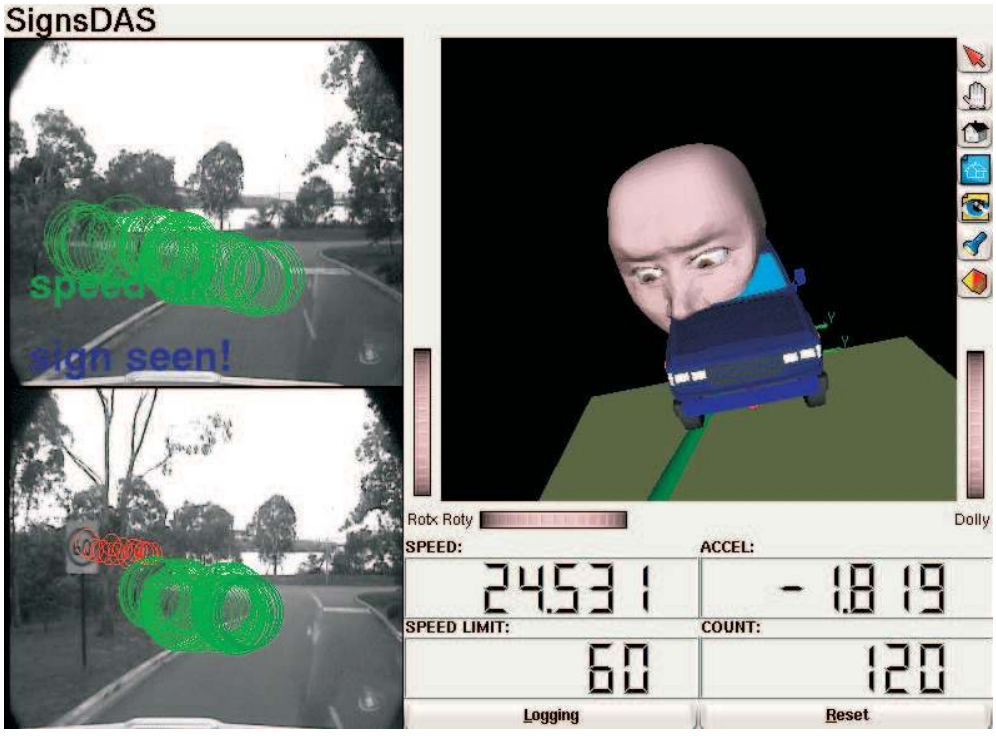

Fig. 20. Screen-shot showing "60" sign detected and seen by driver. Top left: Live video showing eye gaze (large circles) and status (overlaid text). Bottom left: Last detected sign (small circles) and eye gaze (large circles). Top right: 3D model of current vehicle position, eye gaze (oversize head) and sign location. Bottom right: Current detected speed limit, vehicle speed, acceleration and count down for speeding grace period in frames.

since detected. This includes all frames from when the sign was first detected before the sign was able to be verified or classified. Similarly, the faceLAB^{TM} data provides the historical head pose and gaze direction. When a sign has been classified, the sign angles and gaze directions are checked back in time to when the sign was first detected. If the angles from any previous frame fall within the tolerance, the sign is reported as being seen by the driver. If the angles never coincide, the sign is reported as missed. The system provides a 4 second tolerance for the driver to achieve the speed limit. The timer is instigated when the measured speed exceeds the limit and the measured acceleration is not significantly decreasing.

On-road Trials

The system was able to detect speed signs around the University and evaluate the implications for the driver. Figure 20 shows a screen-shot of the system demonstrating a typical case. Figures 21 and 22 illustrate the primary scenarios encountered. In Figure 21(a) the driver was watching a pedestrian and failed to notice a "40" sign. The Automated Co-driver has detected that the driver did not see the sign and has issued a red *sign: missed!* warning. Figure 21(b) shows an instance where an "80" sign was detected; the driver saw the sign and the vehicle was not speeding so no red warning was issued. Similarly, in Figure 22(a) a "40" sign was detected. The driver saw the sign, the system assumed the driver was intentionally speeding so a warning was displayed but no sound alert generated. In Figure 22(b) the driver has missed the last sign and is speeding for more than a predefined grace period without decelerating. The *SLOW DOWN!* warning is shown and an alert sound issued.

Figure 23 shows the sign and the gaze direction separation angle for typical signs classified as "seen" by the system. Note the troughs in the separation angle graphs reflecting times when the driver looked toward the sign.

At one location in the test area there was a speed sign just past an entry road to the University. Due to the intersection geometry and a bend shortly along the entry road the road sign, while in plain view on the road shoulder, was not prominent. After passing the sign the drivers were asked whether they saw the sign, and none of them did. Figure 24 shows the sign and the gaze direction separation angle for three test drivers. The system classifies these signs as missed. Notice the lack of di-

(a) '40' missed. (b) '80' seen.

Fig. 21. The two columns are typical cases for the speed sign inattention system when the vehicle was not speeding. (a) The system detected that the driver most likely missed the road sign. (b) The driver most likely observed the sign. Top row: Live video feeds showing current view, eye gaze (dots/large circles) and current status (overlaid text) during screen-shot. Bottom row: Last detected signs (small circles) and eye gaze during detection (dots/large circles). The small circles on the hood and in the sky in the bottom row are due to a rendering bug at the time of test. They coincide with stale returns that had a strong momentary circular return but failed classification.

rected gaze toward the sign, instead gaze is steady on the road and merging traffic to the right.

In Figure 25 some border line sign gaze angle separation cases are shown. There appears to be some directed eye movement but the angle is greater than the angle error tolerance. Watching the gaze and sign detection it becomes obvious that the sign may be read well before the sign is detectable in the image. The driver eye with much better acuity than the video camera can recognize the sign further away.

To address this case we projected the sign position back according to the recent vehicle egomotion. The sign–gaze separation angle was then taken as the minimum distance to this path. Figure 26 shows the projected paths and the revised sign–gaze angle separation. Now we see that Figures 26(a) and (b) are classified as seen and (c) remains classified as missed. Similar to Figure 24, in Figure 26(c) the sign is on a bend in the road so the sign location remains on the left of the camera image.

For completeness we include Figures 27 and 28 showing the impact of the back projection of the "seen" and "missed" signs. The classifications remain unchanged.

4.5. Multiple Road Event Inattention Detection

The final experiment is an integration of the subsystems outlined above. That is, visual monotony estimation, sign reading, lane tracking, vehicle detection and pedestrian detection combined with driver gaze monitoring.

Road Departure Calculation

To determine whether the vehicle will depart the lane we use the intersection of the estimated lane geometry with the Ack-

(a) "40" seen. Car speeding. (b) "40" missed. Car speeding.

Fig. 22. Typical cases for speed the sign inattention system when the vehicle was speeding. Left: Live video feed showing current view, eye gaze (dots/large circles) and current status (overlaid text) during screen-shot. Right: Last detected sign (small circles) and eye gaze (dots/large circles).

erman motion model of the vehicle (see Figure 29). The intersection point provides a time until departure estimate assuming that the driver maintains the current steering angle. To find this point we solve the lane model and Ackerman equations numerically to find the arc length to departure and, for a known speed, the time until departure.

To determine whether a lane departure is intentional we use the departure point, the turning indicators and the driver eye gaze. If the turning indicators are operating and the lane departure point is in the same direction the warning is suppressed. The warning is also suppressed if the driver gaze has been sufficiently close to the departure point. If neither of these criteria are met an auditory warning is given.

On-line Road Trials

Now follows some illustrative cases of the combined system. Like all of our systems the interface is for the experimenter not the driver, as audio warnings and gaze cancellation provide the interface to the driver. The application cycles through a decision tree to determine possible alerts. First potential pedestrian collisions, then obstacles then lane departures are verified. Then sign events, inattention, vehicle status and finally monotony events are checked. Alerts are given with unique sounds. Approaching obstacles and pedestrians observed by the driver are not warned, nor are lane departures provided the driver is indicating or has gazed in the departure direction.

Figure 30 shows the Automated Co-driver detecting a speed sign. The vehicle was not speeding so no warning was given. The system detects an acknowledgement when the driver looks at the speedometer anyway.

Figure 31 shows inattention detected by gaze monitoring. A glance back at the road resets the inattention alarm.

In Figure 32 the inattention alarm has been reset although now the driver is speeding. Direct driver observation enabled the system to verify that the speed sign had been observed so a visual warning is given, the auditory alarm is suppressed.

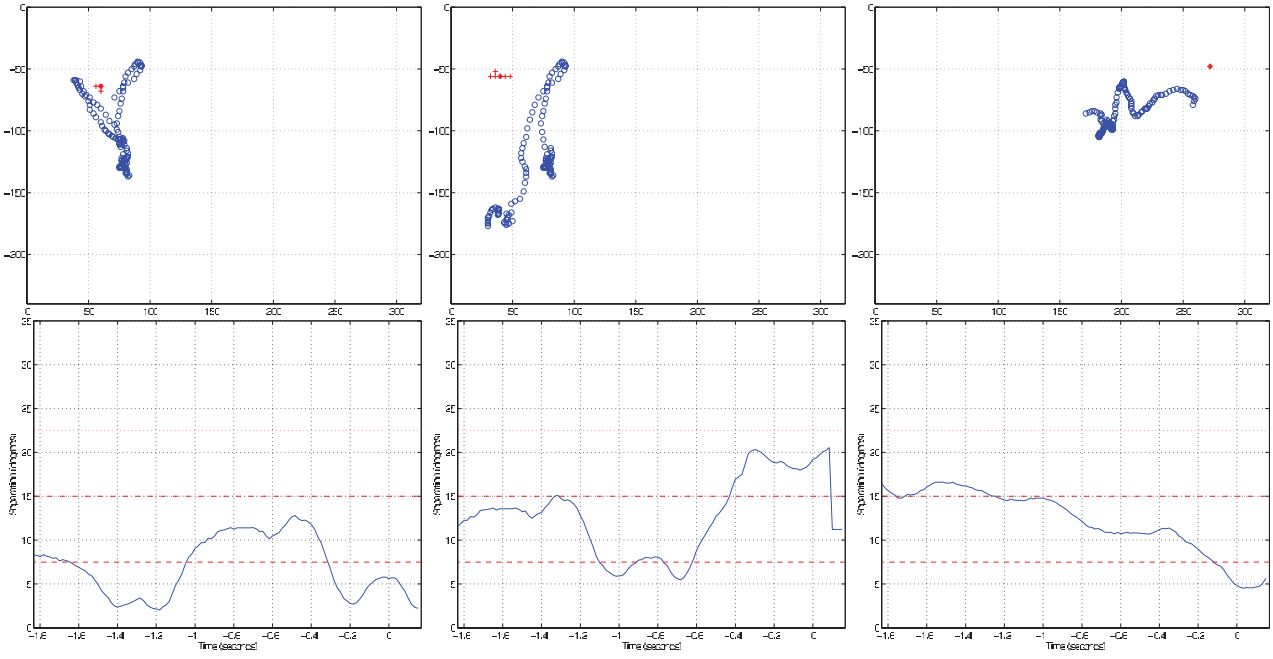

Fig. 23. “Seen” sign, eye-gaze direction separation angle. The origin on the time axis represents the final detection of the sign. Top: (“o”), eye gaze; (“+”), sign position. Bottom: Sign–gaze separation angle. Dashed lines: $1 \times 2 \times 3 \times 7.5^o$ error tolerance.

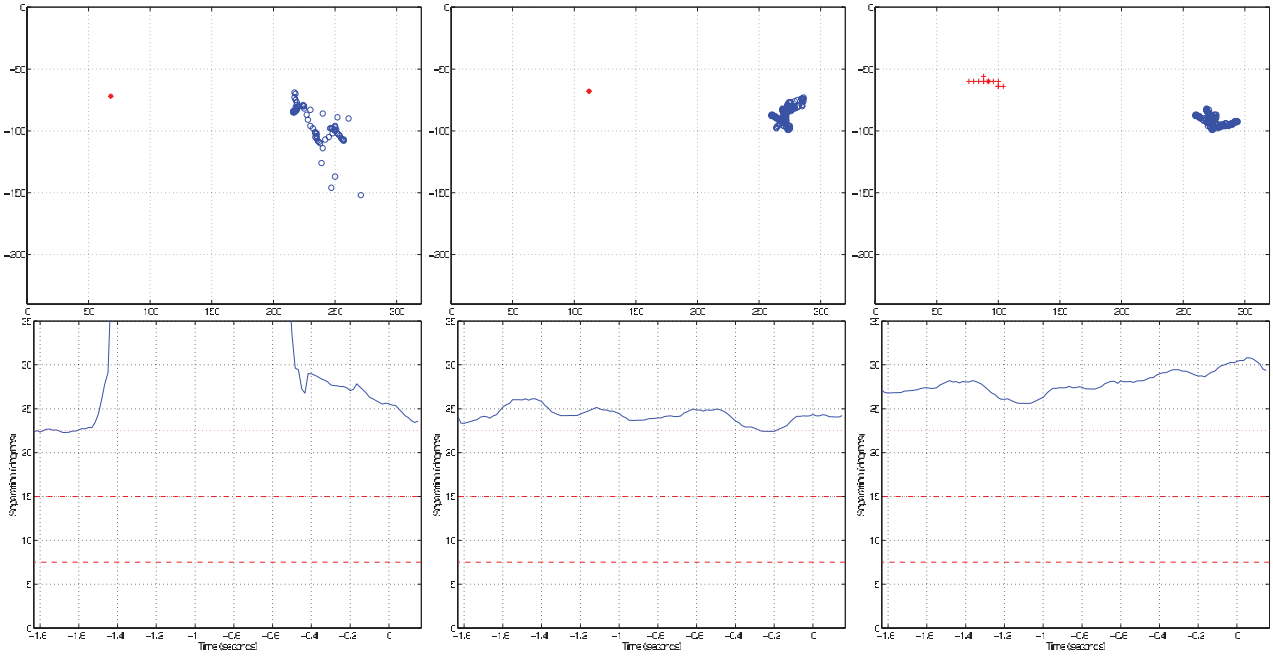

Fig. 24. “Missed” sign, eye-gaze direction separation angle. Top: (“o”), eye gaze; (“+”), sign position. Bottom: Sign–gaze separation angle. Dashed lines: $1 \times 2 \times 3 \times 7.5^o$ error tolerance.

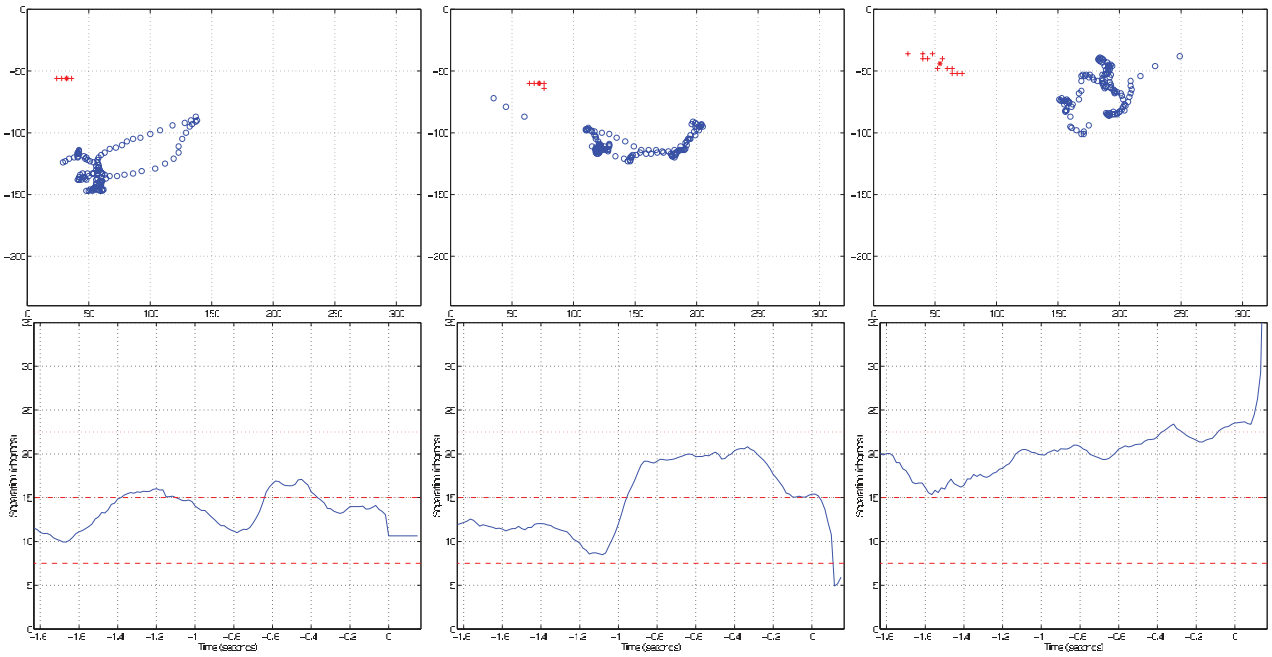

Fig. 25. "Borderline" sign, eye-gaze direction separation angle. Top: ("o"), eye gaze; ("+"), sign position. Bottom: Sign–gaze separation angle. Dashed lines: $1 \times 2 \times 3 \times 7.5^o$ error tolerance.

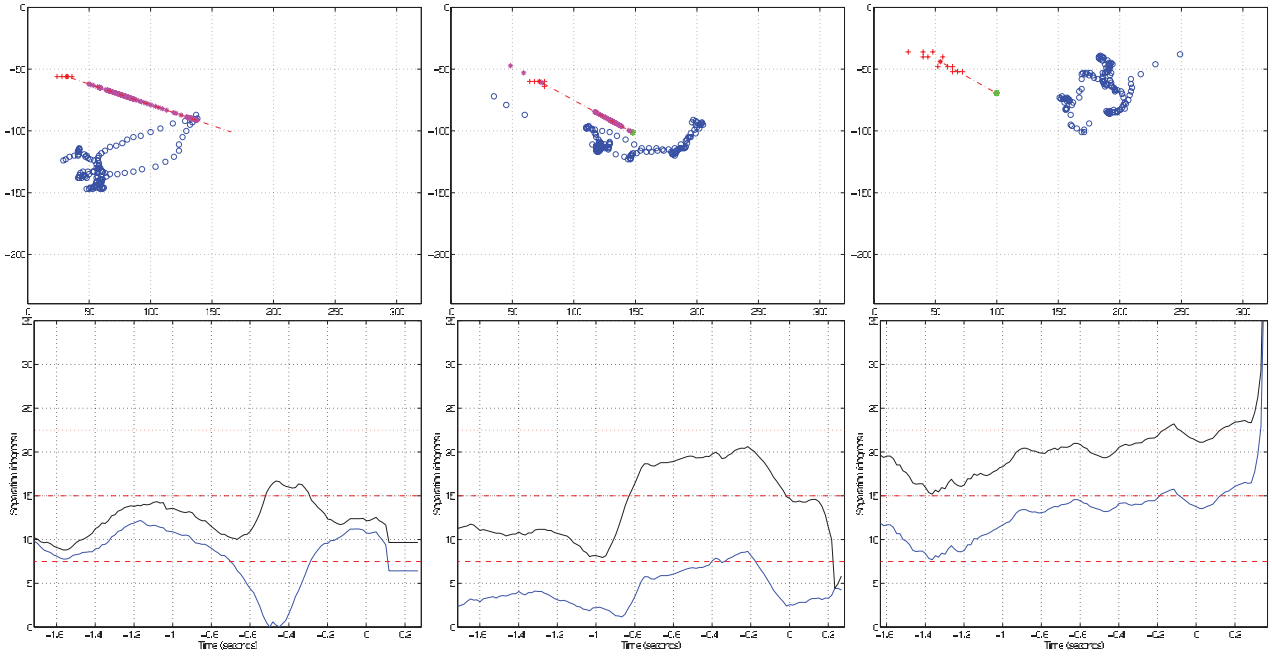

Fig. 26. Sign position projected back in time to estimate sign–gaze direction separation angle before the sign was large enough to track. Top: ("o"), eye gaze; ("+"), sign position; ("*"), projected gaze point on sign path. Bottom: Sign–gaze separation angle. Dark plot: original separation; light plot, back projected separation; dashed lines: $1 \times 2 \times 3 \times 7.5^o$ error tolerance.

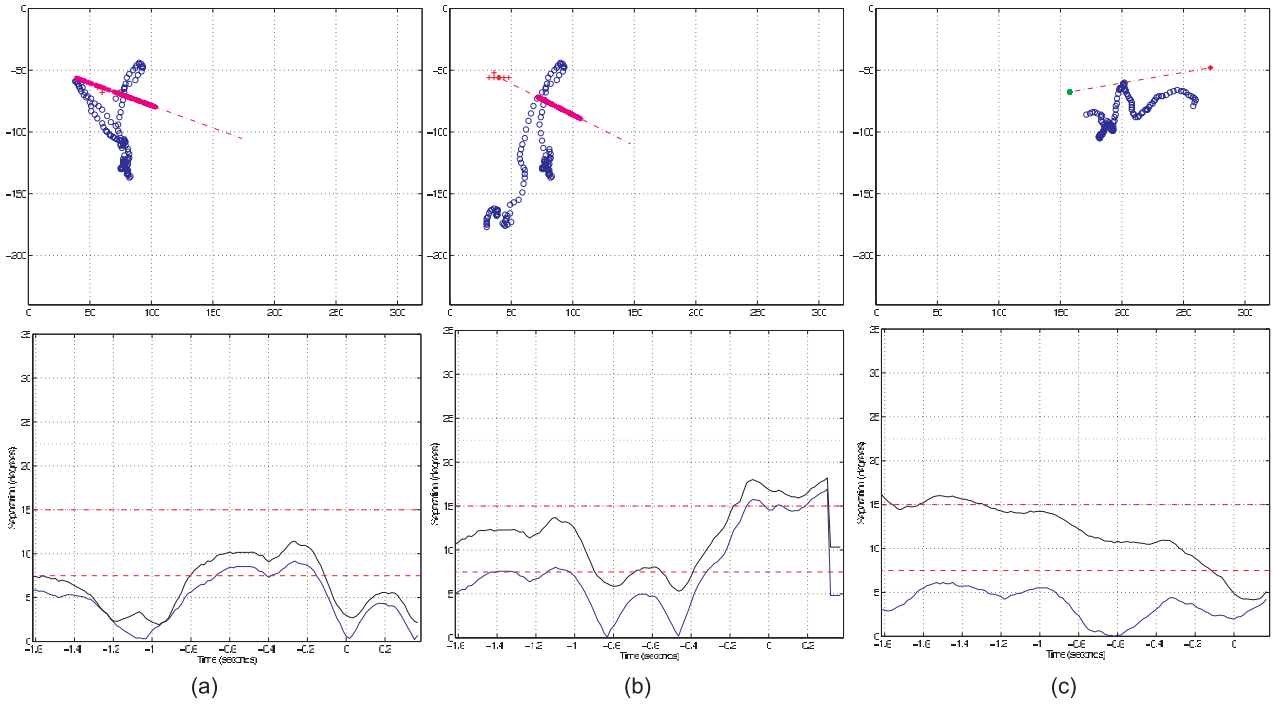

Fig. 27. "Seen" sign, eye-gaze direction separation angle. The origin on the time axis represents the final detection of the sign. Top: ("o"), eye gaze; ("+"), sign position. Bottom: Sign–gaze separation angle. Dark plot: original separation; light plot, back projected separation; dashed lines: $1 \times 2 \times 3 \times 7.5^o$ error tolerance.

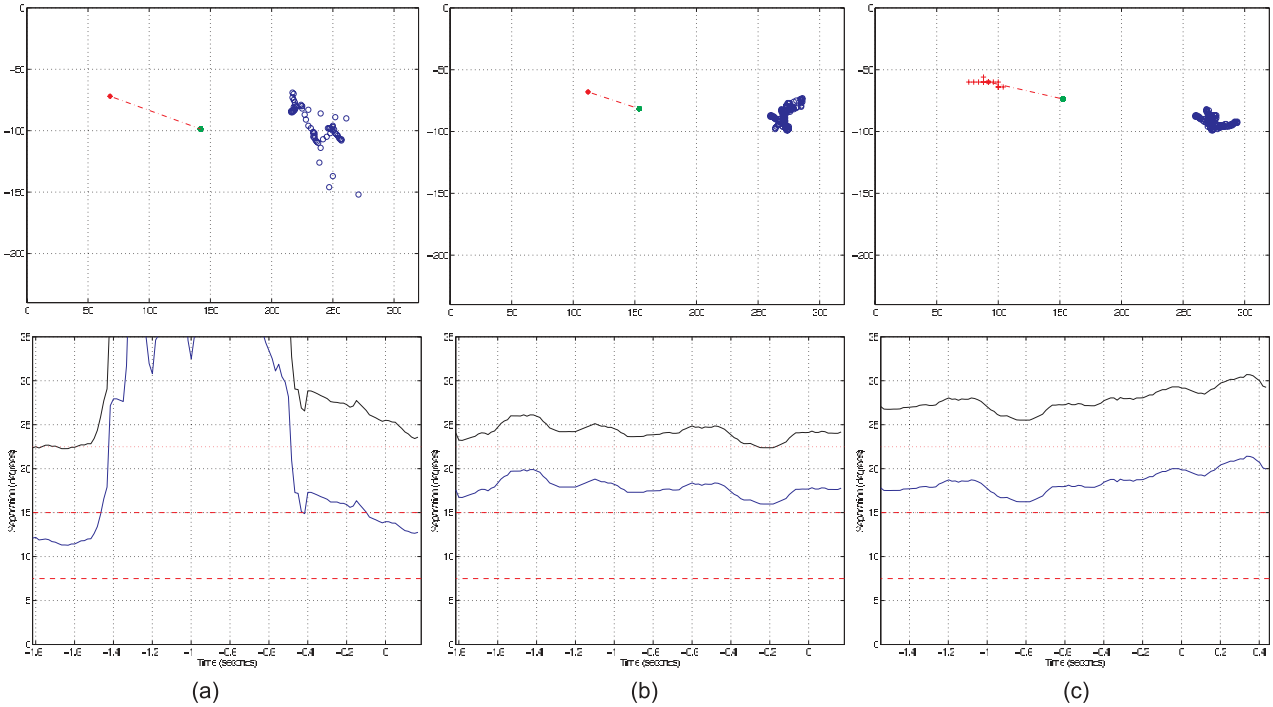

Fig. 28. "Missed" sign, eye-gaze direction separation angle. Top: ("o"), eye gaze; (Red "+"), sign position. Bottom: Sign–gaze separation angle. Dark plot: original separation; light plot, back projected separation; dashed lines: $1 \times 2 \times 3 \times 7.5^o$ error tolerance.

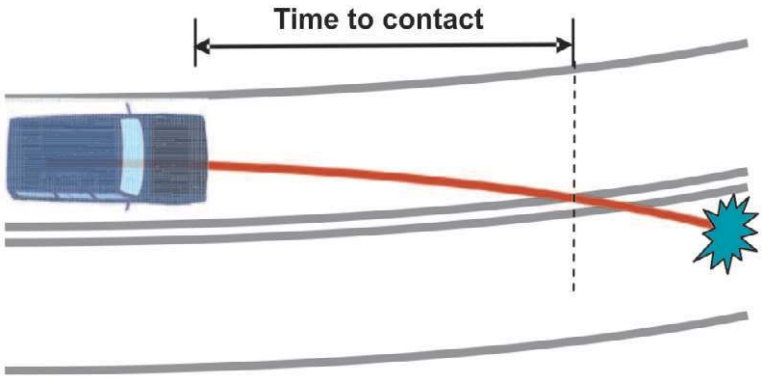

Fig. 29. The current lane departure point is found at the intersection of the estimated lane geometry and the vehicle motion model.

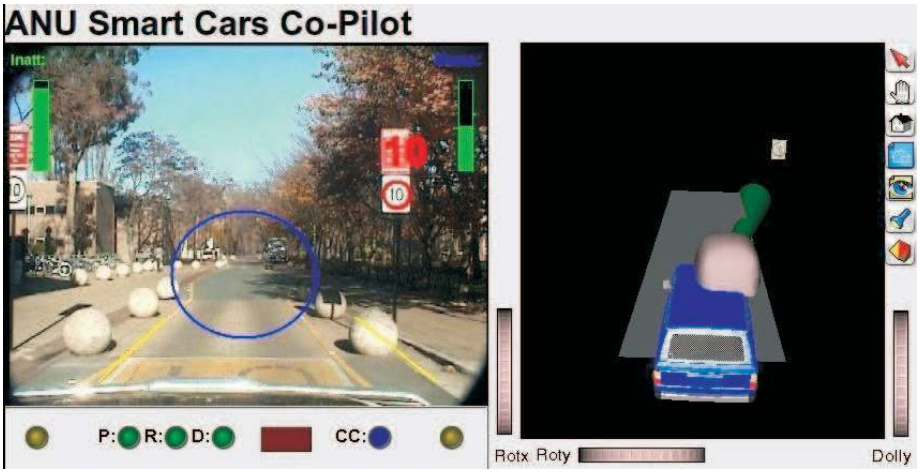

(a)

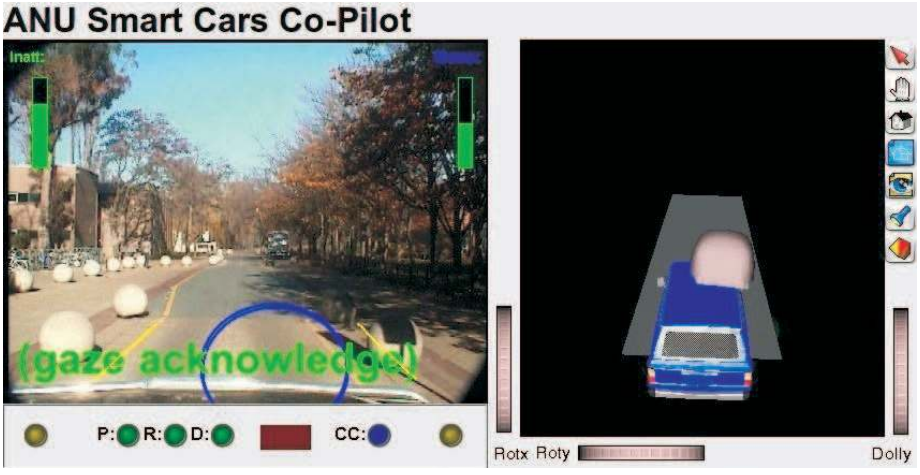

(b)

Fig. 30. Co-driver DAS screen-shot. Circles represent driver gaze. (a) Sign detected. (b) Driver glanced at speedometer.

Fig. 31. Screen-shots of the Automated Co-driver. Prolonged inattention detected. Large circles: no circles are shown in this case as the driver's gaze is outside the field of view of the camera (consistent with the driver inattention detected).

Fig. 32. Screen-shots of the Automated Co-driver. Vehicle speeding, although last speed sign was observed by the driver. Large circles: driver gaze.

Fig. 33. A sequence of screen-shots of the Automated Co-driver. A lane departure that was seen by the driver is shown. Large circles: driver gaze.

Figures 33 and 34 demonstrate cases of detected lane departures. Direct driver observation enables the Automated Co-driver to permit the driver to depart the lane in the sequence in Figures 33.

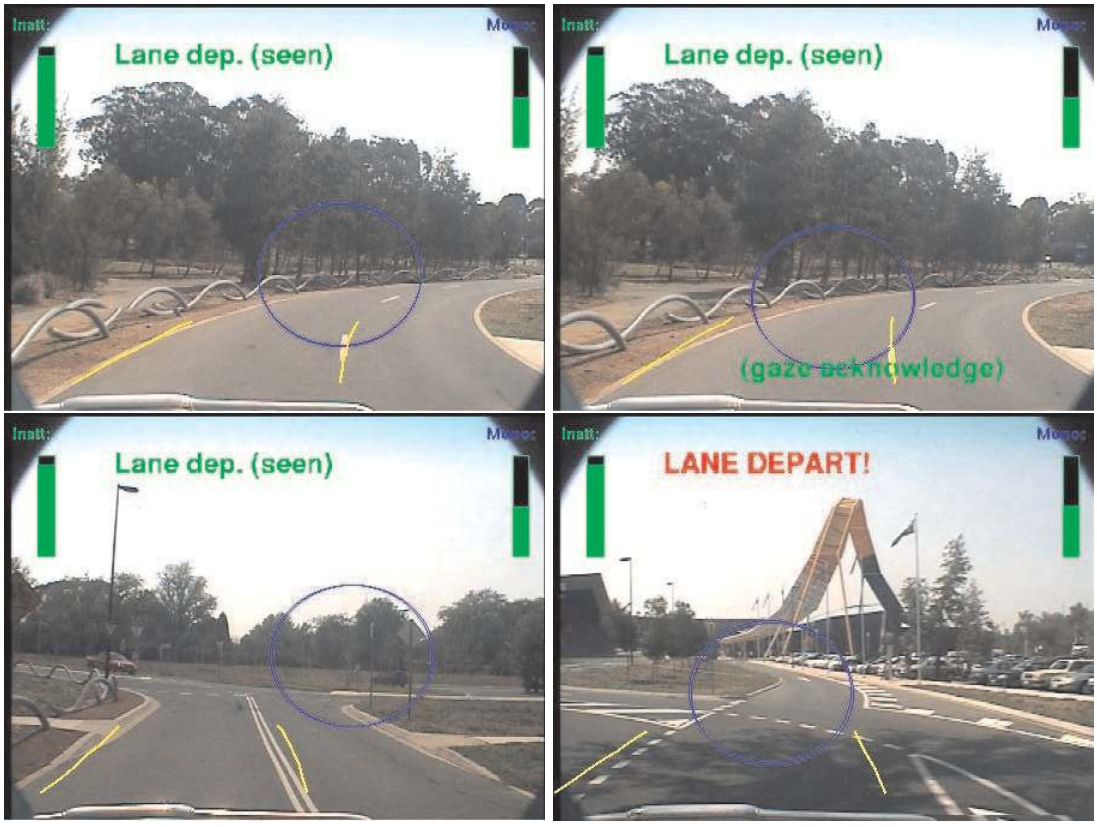

Fig. 34. Screen-shots of the Automated Co-driver. Lane departure warnings. The final case shows when the driver was turning a corner without indicating or looking in the departure direction. Large circles: driver gaze.

(a) (b)

Fig. 35. Automated Co-driver screen-shot sequence. Circles represent driver gaze. (a) Approaching pedestrian detected. (b) Pedestrian determined to be no threat. Arrow added manually afterwards.

Figure 34 shows several cases of intentional lane departure. The final case shows a lane departure without eye-gaze verification. The driver is turning left but has not indicated or looked in that direction. Direct driver observation enables us to detect this final case without having to warn the driver during the first three intentional cases.

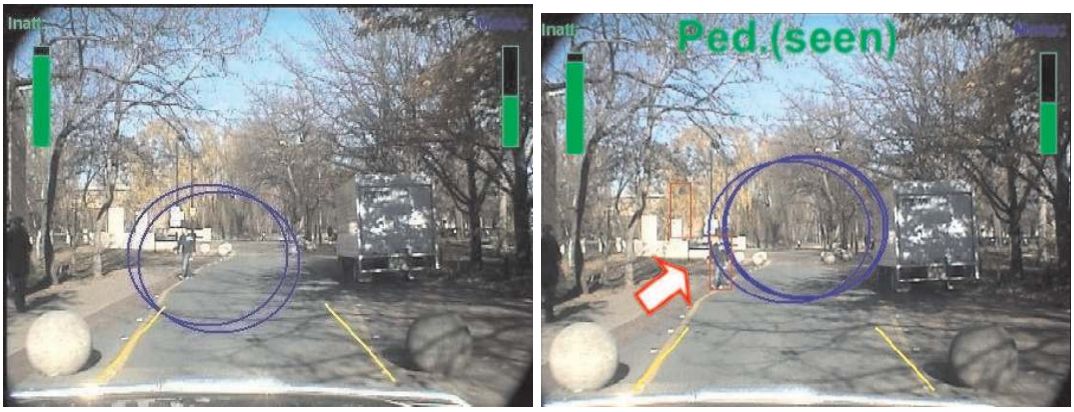

Fig. 36. (a) Approaching pedestrian detected. (b) Pedestrian seen by driver. Arrow added manually afterward.

Fig. 37. Sequence of screen-shots of the Automated Co-driver showing a monotony warning occurring. Large circles: driver gaze.

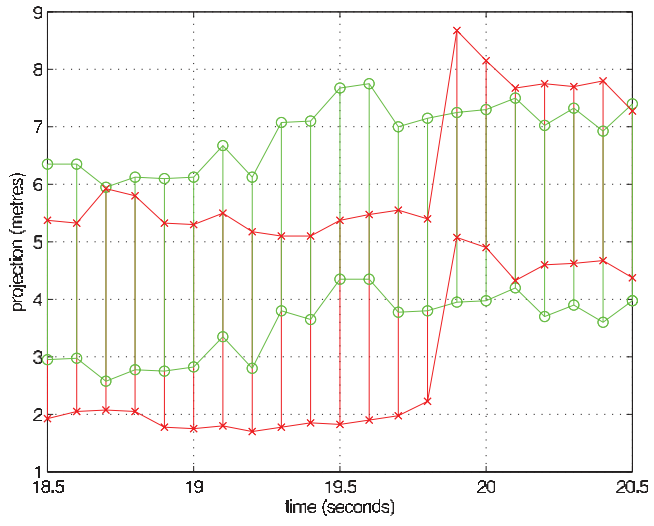

(a)

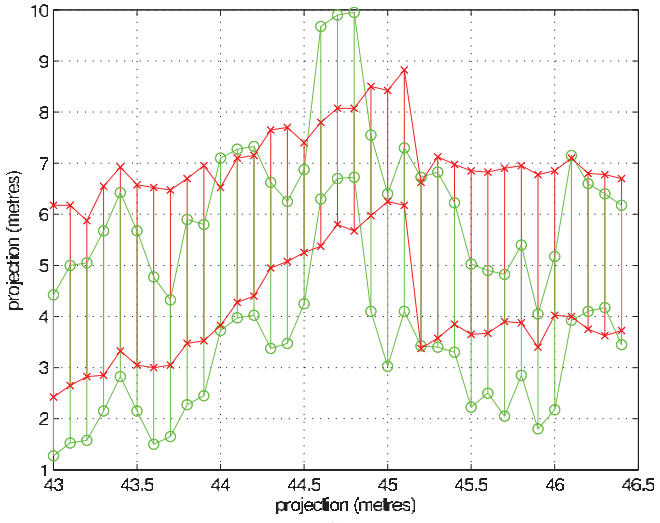

(b)

Fig. 38. (a) Gaze change at 19.3 seconds then intended lane change at 19.9 seconds. (b) Gaze change at 44.9 seconds then intended lane change at 45.3 seconds. (Green "o" and lines), sampled gaze error extents projected onto ground plane; (Red "x" and lines), sampled lane position and width.

Figures 35 and 36 show cases where direct driver observation enabled the system to verify that the pedestrian threat had been observed, so an alert could be suppressed.

Finally, Figure 37 demonstrates a case of a visually monotonous stretch of highway. Visual monotony is detected after several minutes of monotonous road conditions. A visual alert is given indicating the heightened fatigue risk in this scenario. The monotony is broken as the driver approaches a slower vehicle.

Figure 38 shows the lane estimate with gaze direction projected onto the ground plane. In these cases the driver eye

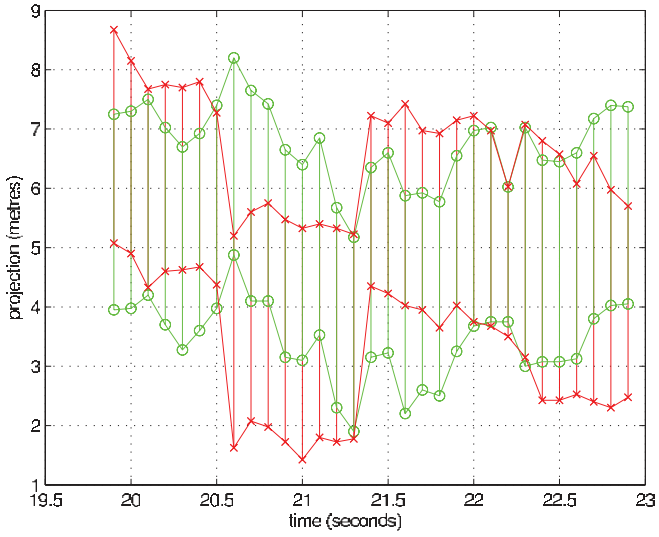

Fig. 39. Unintended lane change. No discernable gaze change to correlate with lane change at 20.6 seconds. Driver reverts to the original lane at 21.4 seconds. (Green "o" and lines), sampled gaze error extents projected onto ground plane, (Red "x" and lines), sampled lane position and width.

gaze shifts focus to the destination lane before the lane change. These cases are detected as intended lane changes.

In contrast Figure 39 shows an unintended lane change. The vehicle moves into the adjacent lane without an eye-gaze transition. The system reports this case as an unintended lane departure. The driver then corrects lane position bringing the vehicle back into the original lane.

Strong direct sunlight caused some uncertainty in the lane tracking and, at times, even disrupted the gaze tracking. When gaze tracking was strong and the driver was attentive at the lane center, uncertainty in the road scene vision did not warrant a warning.

Due to the safety requirements of the vehicle the trial drivers were staff and students of the group but not specifically of this research. The constraint made it hard to detect genuine inattentive behaviour. Nonetheless, the system performed as intended during the trials and did produce occasional warnings during other times which were likely to be genuine warnings of inattentiveness.

5. Conclusion

Observing the complementary strengths and weaknesses of humans and autonomous systems, it is reasonable that an integration of the two provides the best hope to improve road safety, thus combining the flexibility and frailty of human drivers with the tirelessness and inflexibility of automated systems. Our conjecture was that a system capable of estimating what the

driver has seen (the driver's observations) is key to addressing driver inattention – a common underlying factor in many road fatalities.

The use of driver eye gaze combined with road events to estimate the to driver's observations was developed and the feasibility of the approach was verified. Due to the "looking but not seeing" case, it is not possible to determine that road events are seen for certain by the driver. However, it was shown that road events almost certainly missed by the driver could be identified.

The systems correlate the driver eye gaze with road scene events to estimate the driver's observations. The benefit of driver observation monitoring was also demonstrated to suppress redundant warnings and cancel warning "with a glance". These systems have the potential to provide the detection or earlier warning of missed road events. The timely knowledge of these missed events would hopefully provide the precious extra seconds for human reaction time.

References

Amditis, A. et al. (2006). System architecture for integrated adaptive HMI Solutions. *Proceedings of IEEE Intelligent Vehicles Symposium*. June, pp. 388–393.

Apostoloff, N. and Zelinsky, A. (2004). Vision in and out of vehicles: integrated driver and road scene monitoring. *International Journal of Robotics Research*, **23**(4-5): 513–538.

ATSB (2004). Australian Transport Safety Bureau, Serious injury due to road crashes: road safety statistics report. *Technical Report*, Australian Government.

ATSB (2006). Australian Transport Safety Bureau, Fatal Road Crash Database. *http:www.atsb.gov.auroadfatal_road_crash_database.aspx*.

Bertozzi, M., Broggi, A. and Fascioli, A. (2000). Vision-based intelligent vehicles: State of the art and perspectives. *Robotics and Autonomous Systems*, **32**: 1–16.

Carsten, O. and Tate, F. (2001). Intelligent speed adaptation: The best collision avoidance system? *Proceedings of the 17th International Technical Conference on the Enhanced Safety of Vehicles*, June, Amsterdam.

DARPA (2004). Defense Advanced Research Projects Agency, Grand Challenge 2004. http://www.darpa.mil/grandchallenge04/index.htm.

DARPA (2005). Defense Advanced Research Projects Agency, Grand Challenge 2005. http://www.darpa.mil/grandchallenge05/index.htm.

DARPA (2007). Defense Advanced Research Projects Agency, Grand Challenge 2007. http://www.darpa.mil/grandchallenge.

Dickmanns, E. D. and Graefe, V. (1988a). Applications of dynamic monocular machine vision. *Machine Vision and Applications*, **1**(4): 241–261.

Dickmanns, E. D. and Graefe, V. (1988b). Dynamic monocular machine vision. *Machine Vision and Applications*, **1**(4): 223–240.

Fletcher, L., Petersson, L., and Zelinsky, A. (2005a). Road Scene Monotony Detection in a Fatigue Management Driver Assistance System. *Proceedings of the IEEE Intelligent Vehicles Symposium*.

Fletcher, L. et al. (2005b). Correlating driver gaze with the road scene for driver assistance systems. *Robotics and Autonomous Systems*, **52**(1): 71–84.

Franke, U. et al. (1998). Autonomous driving approaches downtown. *IEEE Intelligent Systems*, **9**(6): 40–48.

Franke, U. and Heinrich, S. (2002). Fast obstacle detection for urban traffic situations. *IEEE Transactions on Intelligent Transportation Systems*, **3**(3): 173–181.

Gerdes, J. C. and Rossetter, E. J. (2001). A unified approach to driver assistance systems based on artificial potential fields. *Journal of Dynamic Systems, Measurement and Control*, **123**(3): 431–438.

Gordon, A. D. (1966). Perceptual basis of vehicular guidance. *Public Roads*, **34**(3): 53–68.

Grubb, G. and Zelinsky, A. (2004). 3D vision sensing for improved pedestrian safety. *Proceedings of the IEEE Intelligent Vehicles Symposium*. June, pp. 19–24.

Haworth, N. L., Triggs, T. J. and Grey, E. M. (1988). Driver fatigue: Concepts, measurement and crash countermeasures. *Technical Report*, Federal Office of Road Safety Contract Report 72, Human Factors Group, Monash University, Department of Psychology.

Holzmann, F. et al. (2006). Introduction of a full redundant architecture into a vehicle by integration of a virtual driver. *Proceedings of the IEEE Intelligent Vehicles Symposium*, June, pp. 126–131.

Hsu, S.-H. and Huang, C.-L. (2001). Road sign detection and recognition using matching pursuit method. *Image and Vision Computing*, **19**: 119–129.

Isard, M. and Blake, A. (1996). Contour tracking by stochastic propagation of conditional density. *Proceedings of the European Conference on Computer Vision*, April, Vol. 1, pp. 343–356.

Ishikawa, T., Baker, S. and Kanade, T. (2004). Passive driver gaze tracking with active appearance models. *Proceedings of the 11th World Congress on Intelligent Transportation Systems*. October.

Labayrade, R., Aubert, D. and Tarel, J.-P. (2002). Real time obstacle detection in stereovision on non flat road geometry through v-disparity representation. *Proceedings of the IEEE Intelligent Vehicle Symposium*, France, June, pp. 646–651.

Land, M. and Lee, D. (1994). Where we look when we steer. *Nature*, **369**(6483): 742–744.

Loy, G. and Zelinsky, A. (2003). Fast radial symmetry for detecting points of interest. *IEEE Transactions on Pattern Analysis and Machine Intelligence*, **25**(8): 959–973.

Maltz, M. and Shinar, D. (2004). Imperfect in-vehicle collision avoidance warning systems can aid drivers. *Human Factors*, **46**(2): 357–366.

Matsumoto, Y., Heinzmann, J. and Zelinsky, A. (1999). The essential components of human-friendly robots. *Proceedings of the International Conference on Field and Service Robotics FSR'99*, August, pp. 43–51.

Neale, V. L. et al. (2005). Overview of the 100-Car Naturalistic study and findings. *Proceedings of the International Conference on Enhanced Safety of Vehicles*, June.

OECD (2006). Organisation for Economic Co-operation and Development, Factbook 2006 – Economic, Environment and Social Statistics: Quality of life. http://www.sourcecd.org, December.

OECD/ECMT (2006). Ambitious Road Safety Targets and the Safe System Approach, OECD Publishing.

Pomerleau, D. and Jochem, T. (1996). Rapidly adapting machine vision for automated vehicle steering. *IEEE Expert: Special Issue on Intelligent Systems and their Applications*, **11**(2): 19–27.

Rasolzadeh, B., Petersson, L. and Pettersson N. (2006). Response binning: improved weak classifiers for boosting. *Proceedings of the IEEE Intelligent Vehicles Symposium*, June, pp. 344–349.

Regan, M. A. (2005). Keynote address. *Proceedings of the Australasian College of Road Safety (acrs), NSW Joint parliamentary standing committee (Staysafe) International Conference on Driver Distraction*, June, pp. 29–73.

Seeing Machines (2001). FaceLAB: A face and eye tracking system. http:www.seeingmachines.com.

Stutts, J. et al. (2001). The role of driver distraction in traffic crashes. *Technical Report*, Foundation for Traffic Safety, USA.

Summala, H. and Nicminen, T. (1996). Maintaining lane position with peripheral vision during in-vehicle tasks. *Human Factors*, **38**: 442–451.

Takemura, K. et al. (2003). Driver monitoring system based on non-contact measurement system of driver's focus of visual attention. *Proceedings of the IEEE Symposium on Intelligent Vehicles*, June, pp. 581–586.

Thiffault, P. and Bergeron, J. (2003). Monotony of road environment and driver fatigue: a simulator study. *Accident Analysis and Prevention*, **35**: 381–391.

Thrun, S. et al. (2006). Stanley: the robot that won the DARPA Grand Challenge. *Field Robotics*, **23**(9): 661–692.

Treat, J. et al. (1979). Tri-level study of the causes of traffic accidents: final report – executive summary. *Technical Report DOT-HS-034-3-535-79-TAC(S)*, Institute for Research in Public Safety, University of Indiana, USA.

Trivedi, M. M., Gandhi, T., and McCall, J. (2005). Looking-in and looking out of a vehicle: selected investigations in computer vision based enhanced vehicle safety. IEEE International Conference on Vehicular Electronics and Safety, October, pp. 29–64.

Victor, T. (2005). *Keeping eye and mind on the road. Ph.D. Thesis*, Department of Psychology, Uppsala University, Sweden.

Viola, P., Jones, M. J. and Snow, D. (2005). Detecting pedestrians using patterns of motion and appearance. *International Journal of Computer Vision*, **63**(2): 153–161.

Wandell, B. A. (1995). *Foundations of Vision*. Sunderland, USA, Sinauer Associates.

WHO (2001). World health report. *Technical Report*, World Health Organisation, http://www.who.int/whr2001/2001/main/en/index.htm.